Table 1 Histological findings of azoxymethane-induced colon polyps in adiponectin-deficient (KO) mice and wild-type (WT) mice receiving a high-fat diet

Experimental group	Adenocarcinoma	Adenoma	Total
WT (n = 10)	15 (42%)	21 (58%)	36 (100%)
KO (n = 10)	51 (60%)	34 (40%)	85 (100%)

MATERIALS AND METHODS

Animal models

All mice were treated humanely in accordance with the National Institutes of Health and AERI-BBRI Animal Care and Use Committee guidelines. Adiponectin (ACRP30 or AdipoQ)-deficient (*ACRP30−/−*) mice (KO mice) and adiponectin receptor 1 or 2-deficient mice (*AdipoR1−/−* or *AdipoR2−/−*) were generated by our group as described previously.[21] We performed the experiments in this study using littermate mice backcrossed to C57Bl/6 for 10 generations.

The animals were fed a basal diet or a high-fat diet until the end of the study. The composition of both diets is listed in supplementary table 1. Three to five mice were housed per metallic cage with sterilised softwood chips as bedding, in a barrier-sustained animal room air-conditioned at 24 (SD 2)°C and 55% humidity, under a 12 h light–dark cycle.

Induction of colon polyps

Azoxymethane (AOM) was purchased from Sigma (St. Louis, Missouri, USA). Mice (6 weeks old) were divided into four groups: (1) WT mice fed the basal diet (n = 10), (2) KO mice fed the basal diet (n = 10), (3) WT mice fed the high-fat diet (n = 10), and (4) KO mice fed the high-fat diet (n = 10). Mice were injected intraperitoneally with 10 mg/kg of AOM once a week for 6 weeks and sacrificed at 20 weeks following initiation of AOM injection to evaluate the difference in the extent of polyp formation between the KO and WT mice (supplementary fig 1A).

Induction of aberrant crypt foci

Mice (6 weeks old) were divided into four groups: (1) WT mice fed the basal diet (n = 12 mice), (2) KO mice fed the basal diet (n = 11), (3) WT mice fed the high-fat diet (n = 11), and (4) KO mice fed the high-fat diet (n = 11). Mice were given two weekly intraperitoneal injections of 10 mg/kg of AOM and sacrificed at 6 weeks following initiation of AOM injection (supplementary fig 1B). The protocol of the 2-amino-1-methyl-6-phenylimidazo-[4,5-*b*]pyridine (PhIP)-induced aberrant crypt foci (ACF) model is shown in supplementary fig 2A.[29]

Effect of the AMP kinase activator and mTOR inhibitor on colon carcinogenesis

The AMP kinase activator 5-aminoimidazole-4-carboxamide-1-β-D-ribofuranoside (AICAR) and the mTOR inhibitor rapamycin were purchased from BIOMOL (Plymouth Meeting, PA, USA). WT and KO mice (6 weeks old) were intraperitoneally injected with AICAR (0.1 mg/kg/day), rapamycin (0.2, 0.4, 0.8 mg/kg) or vehicle (saline) until the end of the experiment. The mice in each group were fed the high-fat diet and received AOM injections according to the ACF protocol.

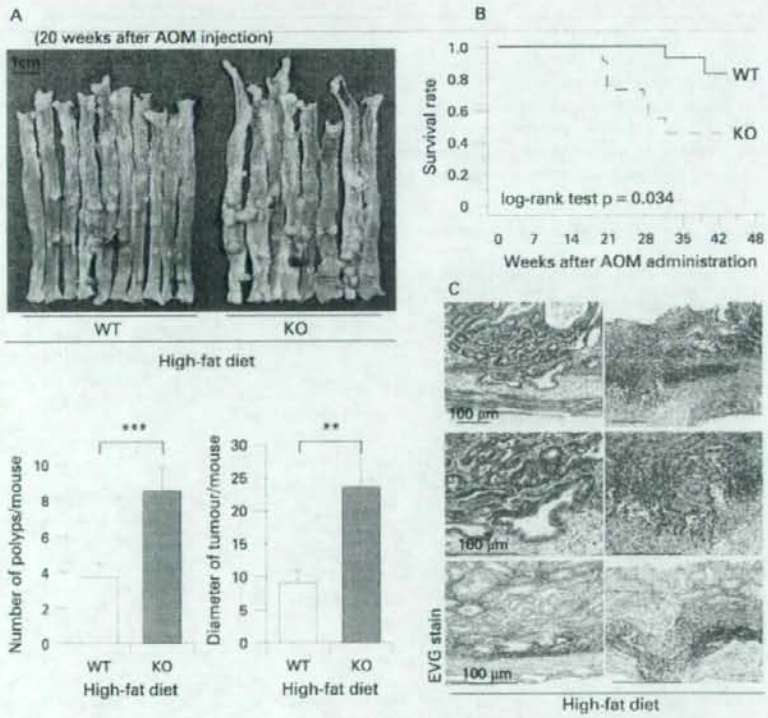

Figure 1 Promotion of colon polyp formation in adiponectin-deficient (KO) mice under the high-fat diet condition. (A) Upper panel: Macroscopic findings of colon polyp in wild-type (WT) and KO littermate mice under the high-fat diet condition at 20 weeks following initiation of azoxymethane (AOM) injection. Lower panel: Number and diameter of polyps per mouse in the high-fat diet groups. Each column represents the mean (with the SEM), *p<0.05. (B) Survival rate of the WT and KO littermates under the high-fat diet condition. The survival rate of the WT mice (solid line) was significantly higher than that of the KO mice (broken line) under the high-fat diet condition. More than half of the KO mice died by the end of the study, while only two of the WT mice died. (C) Invasive polyps in the colons obtained from the KO mice under the high-fat diet condition. Haematoxylin and eosin staining (upper and middle panels) and Elastica van Gieson staining (EVG stain, lower panel) were performed using samples isolated from three individual animals.

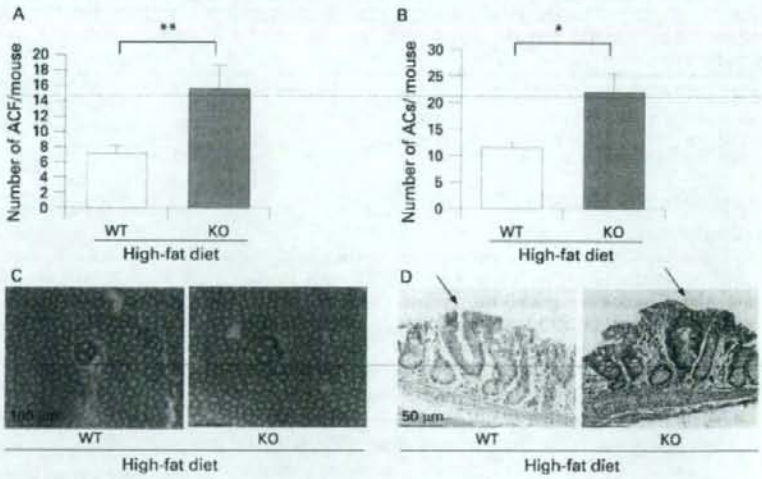

Figure 2 Enhancement of the formation of aberrant crypt foci (ACF) in adiponectin-deficient (KO) mice under the high-fat diet condition. (A,B) Average number of ACF (A) and aberrant crypts (ACs) (B) in the two groups, wild-type (WT) and KO littermate mice, under the high-fat condition, respectively. Each column represents the mean (with the SEM), *p<0.05, **p<0.01. (C) Stereomicroscopic observations of ACF in colon tissue from each group. The samples were stained with 0.2% methylene blue. (D) Representative haematoxylin and eosin staining of ACF in WT and KO mice under the high-fat diet condition.

Histological analysis of the aberrant crypt foci and colon polyps

The entire colon was removed and fixed in 10% neutralised formalin and the numbers of polyps, ACF and aberrant crypts (ACs) were counted as described previously.[10] To facilitate counting, the colons were stained with 0.2% methylene blue solution and observed by stereomicroscopy. After being counted, they were removed and embedded in paraffin blocks according to standard procedures. Paraffin sections were then prepared at 3.0 μm thickness, stained with hematoxylin & eosin and Elastica van Gieson staining for a detection of submucosal invasion, and subjected to histological analysis.

Analysis of the survival rate

In the polyp induction experiment, both the KO (n = 11) and WT (n = 12) mouse groups were continuously observed for 45 weeks. Survival curves were drawn using the Kaplan–Meier method and analysed using the log-rank test.

Assay for assessment of the proliferative activity of the colon epithelial cells

We evaluated the bromodeoxyuridine (BrdU) and the proliferating cell nuclear antigen (PCNA) labelling indices to determine the proliferative activity of the colon epithelial cells. BrdU (BD Biosciences, New Jersey, USA) was diluted in phosphate-buffered saline at 1 mg/ml and administered intraperitoneally at a dose of 50 mg/kg, 1 h prior to the sacrifice of the mice. Immunohistochemical detection of BrdU was performed using a commercial kit (BD Biosciences) and a PCNA detection kit (Zymed Laboratories, South San Francisco, California, USA) was used for PCNA detection. The BrdU and PCNA labelling indices were expressed as the ratio of the number of positively stained nuclei to the total number of nuclei counted in the crypts of the colon. The criteria for selecting the crypts included the presence of a clearly visible and continuous cell column on each side of the crypt. Twenty crypts were evaluated each mouse.

Immunoblotting

The extracted protein was separated by sodium dodecyl sulfate polyacrylamide gel electrophoresis (SDS-PAGE) and the separated proteins were transferred to a polyvinylidene difluoride (PVDF) membrane (Amersham, London, UK). The membranes were probed with primary antibodies specific for adiponectin receptor 1, adiponectin receptor 2 (Santa Cruz Biotech, California, USA), phospho-AMPK, AMPK, phospho-mTOR, mTOR, phospho-S6K, S6K, phospho-S6 protein, S6 protein (Cell Signaling Technology, Danvers, Massachusetts, USA) and glyceraldehyde-3-phosphate dehydrogenase (GAPDH) (Trevigen, Gaithersburg, Maryland, USA). Horseradish-peroxidase-conjugated secondary antibodies and the enhanced chemiluminescence (ECL) detection kit (Amersham) were used for the detection of specific proteins.

Statistical analysis

Statistical analyses for the number of ACF, number of colon polyps, BrdU labelling index and PCNA labelling index were conducted using the Mann–Whitney test. The results for western blot analysis were obtained using the Student t test. Values of $p<0.05$ were regarded as denoting statistical significance.

RESULTS

Promotion of colon polyp formation and lower survival rate in adiponectin-deficient mice under the high-fat diet

The number of polyps in the KO mice was significantly higher than that in the WT mice under the high-fat diet (fig 1A), while there was no difference in the total number of polyps between the WT and KO mice under the basal diet (supplementary fig 3). The sum of the diameter of the polyps per mouse was also measured and similar results were obtained. Table 1 shows histological findings of polyps in mice under high-fat diet. We also observed the survival rate of the WT and KO mice under the high-fat diet condition in the AOM model, and there was a significantly higher survival rate in the WT mice than in the KO mice. While more than half of the KO mice were dead by the end of the study, only two WT mice died (fig 1B).

Interestingly, invasion by malignant cells was observed in parts of the polyps exclusively in the KO mice under the high-fat diet, and the malignant cells were found to have destroyed the muscularis mucosae and invaded the submucosal layer in

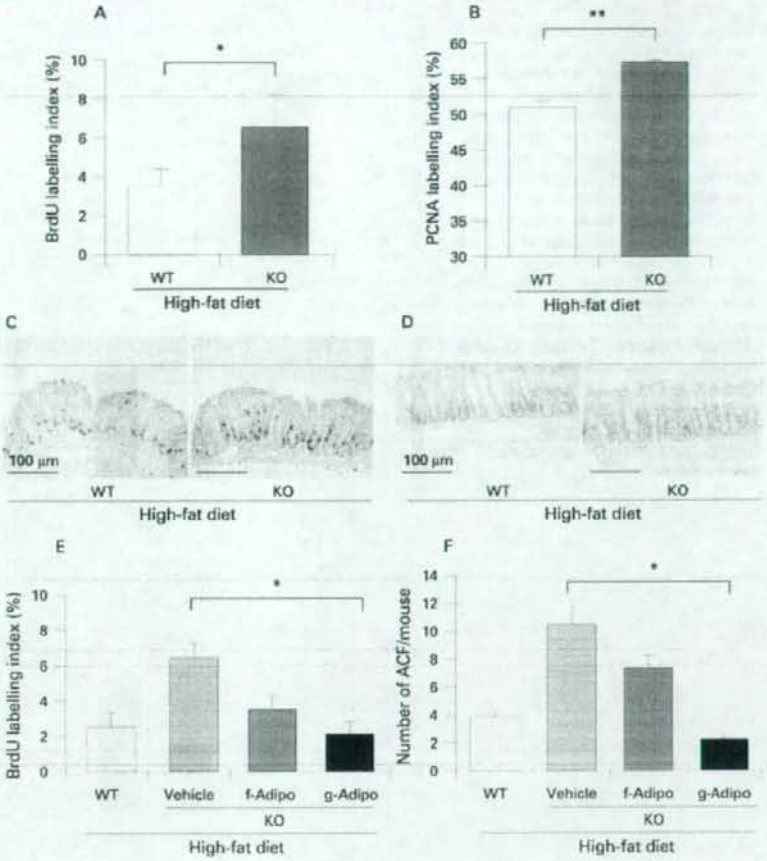

Figure 3 Increase in the colonic epithelial cell proliferative activity in adiponectin-deficient (KO) mice under the high-fat diet condition. (A,B) Average bromodeoxyuridine (BrdU) labelling index (A) and proliferating cell nuclear antigen (PCNA) labelling index (B) in each group in the aberrant crypt foci (ACF) formation experiment. BrdU was administered intraperitoneally 1 h prior to the sacrifice of the animals. Both indices were expressed as the percentage of positively stained nuclei out of the total number of nuclei counted in the crypts of the colon. Each bar represents the mean (with the SEM), *p<0.05, **p<0.01. (C,D) Representative immunohistochemical staining for BrdU (C) and PCNA (D) in each group. (E,F) Wild-type (WT) mice and KO littermate mice fed the high-fat diet were injected intraperitoneally with 50 μg/body recombinant full-length adiponectin (f-Adipo) or 5 μg/body recombinant globular adiponectin domain (g-Adipo) or only vehicle every other day for 6 weeks in an ACF experiment. Adiponectin ameliorates the epithelial cell hyperproliferation in the KO mice under the high-fat diet condition (E). The same effect was observed on the suppression of ACF formation (F).

the tissue specimens (fig 1C), whereas no such invasion was observed in the WT mice. At the end of experiment, the body weight in KO mice was decreased compared to WT mice under the high-fat diet (supplementary fig 4A,B).

Enhanced formation of aberrant crypt foci in adiponectin-deficient mice under the high-fat diet

To investigate the effect of adiponectin in suppressing colon carcinogenesis under the high-fat diet, we analysed colon specimens for the formation of ACF, defined as clusters of aberrant crypts, as a marker of the early stage of colorectal carcinogenesis.[31 32] Although there were no significant differences in the total number of ACF and ACs between the WT and KO littermates mice under the basal diet (data not shown), the numbers of ACF and ACs in the KO mice were significantly higher than those in the WT littermates under the high-fat diet (fig 2A,B). The macroscopic and microscopic characteristics of the ACF in the WT and KO mice under the high-fat diet condition are shown in fig 2C,D; no morphological differences of the ACF were observed between the WT and the KO mice. The differences in the body weight (supplementary fig 4C,D) and the serum levels of adiponectin, glucose, insulin, lipids, and tumour necrosis factor α between the WT and the KO mice are shown in supplementary table 2. In agreement with previous metabolic studies of adiponectin-deficient mice,[33] there were no differences between the two groups under the high-fat diet. To confirm the protective role of adiponectin in colorectal carcinogenesis, the food-borne carcinogen PhIP was used as a second model of colon carcinogenesis in mice fed a high-fat diet. Similar results to those obtained using the AOM-induced carcinogenesis model was obtained (supplementary fig 2).

Increase in cell proliferative activity in adiponectin-deficient mice under the high-fat diet condition

We investigated the proliferative activity of the colon epithelium by determining the BrdU and PCNA labelling indices. Both indices were increased in the KO mice as compared with their WT littermates under the high-fat diet (fig 3A–D). On the other hand, there was no difference under the basal diet (data not shown). Moreover, we examined both indices in colon polyps under the high-fat diet but there was no difference between WT and KO mice (supplementary fig 5).

Adiponectin ameliorates epithelial cell hyper-proliferation in adiponectin-deficient mice under the high-fat diet condition

We administered recombinant adiponectin via an intraperitoneal injection to KO mice in comparison to their WT littermates under the high-fat diet condition. Globular domain adiponectin

Gut 2008;57:1531–1538. doi:10.1136/gut.2008.159293

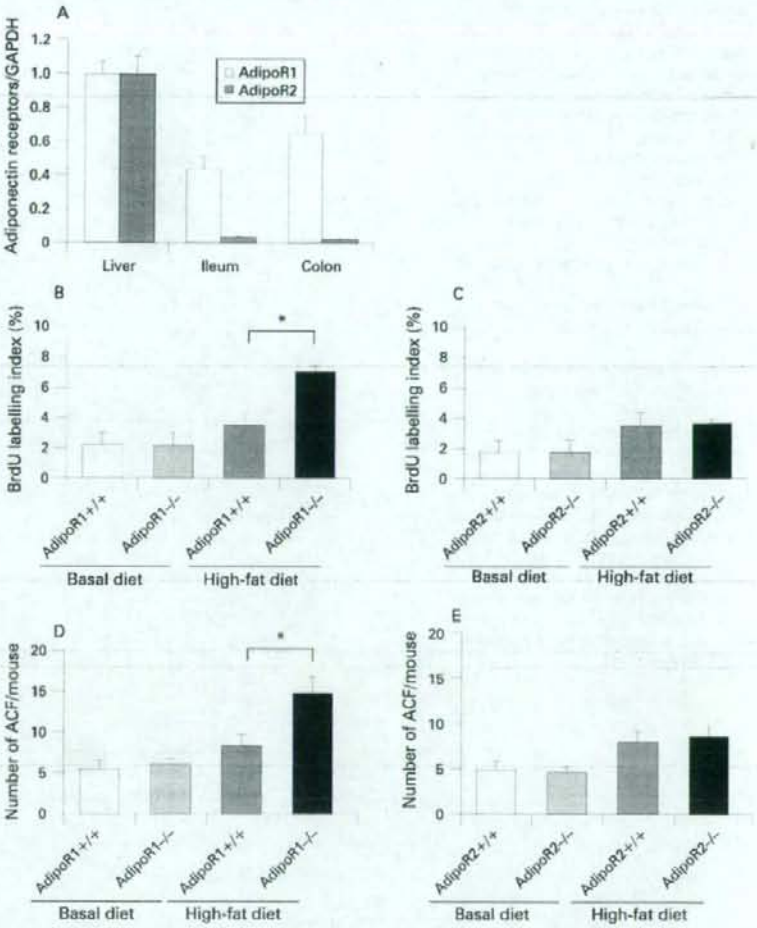

Figure 4 Expression of the adiponectin receptors AdipoR1 and AdipoR2 in the liver, ileum and colon, and promotion of epithelial cell proliferation in AdipoR1−/− mice under high-fat diet condition. (A) Western blot analysis to investigate the expression of AdipoR1 and AdipoR2 was performed on protein obtained from the liver, ileum and colon. The ratio in the liver was defined as 1.0. (B,C): Average bromodeoxyuridine (BrdU) labelling index on colon epithelium from AdipoR1−/− and AdipoR2−/− mice in comparison to the wild-type (WT) littermate mice under basal and high-fat diet condition. The increase in the epithelial cell proliferation was observed in AdipoR1−/− mice, but not in AdipoR2−/− mice under the high-fat diet condition. (D,E) Average number of aberrant crypt foci (ACF) in AdipoR1−/− (D) and AdipoR2−/− mice (E). GADPH, glyceraldehyde-3-phosphate dehydrogenase.

exerted a more potent effect on the suppression of proliferative activity of colon epithelial cells than full-length adiponectin under the high-fat diet (fig 3E). The same effect was observed on the suppression of ACF formation (fig 3F).

The increase in cell proliferative activity in adiponectin receptor 1-deficient mice under the high-fat diet

By using western blot analyses we investigated whether adiponectin receptors are expressed in the colon epithelium, and observed that AdipoR1 was predominantly expressed in the colon in comparison to AdipoR2 (fig 4A).

The BrdU index in the *AdipoR1*−/− mice was significantly higher than in their WT littermates under the high-fat diet (fig 4B). The numbers of ACF and ACs in the *AdipoR1*−/− mice were also significantly higher than their WT littermates (fig 4D). However, no difference in BrdU index and the number of ACF was observed in *AdipoR2*−/− mice and their WT littermates (fig 4C,E). These results suggest that the AdipoR1-mediated, but not the AdipoR2-mediated, pathway may play an important role in the suppressive effect of adiponectin on colorectal carcinogenesis under the high-fat diet, not under the basal diet.

The mTOR pathway is relatively activated in the colon epithelium of adiponectin-deficient mice in comparison to wild-type mice under the high-fat diet

In order to clarify the mechanisms underlying the enhanced proliferative activity of the colon epithelial cells in the presence of adiponectin deficiency, we investigated the expression levels of various potential target proteins in colonic specimens prepared from the WT mice and KO mice under the high-fat diet. The results of western blot analysis revealed that the amounts of phosphorylated mTOR, S6 kinase and S6 protein were significantly higher in the KO mice compared with the WT mice under the high-fat diet (fig 5B–D). It has been reported that adiponectin activates AMPK via AdipoR1, and AMPK is known to suppress the mTOR pathway.[20 34] A significant decrease in the level of phosphorylated AMPK was observed in the KO mice compared with that in the WT mice under the high-fat diet (fig 5A). Moreover, adiponectin administration ameliorated activation of the AMPK/mTOR pathway in KO mice under the high-fat diet condition (supplementary fig 6). These results indicate that, under the high-fat diet, deficiency of adiponectin suppresses AMPK activation, which results in

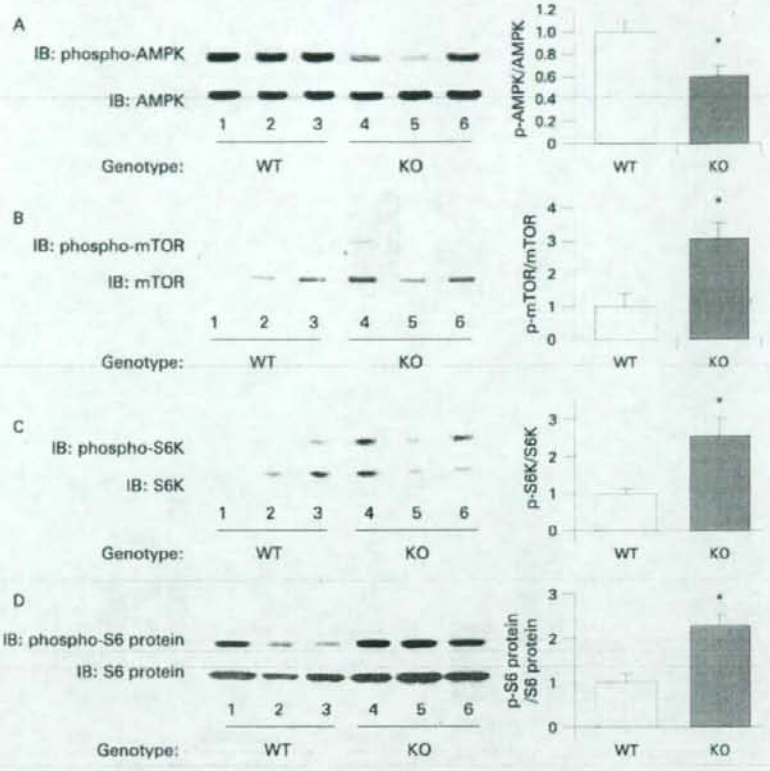

Figure 5 Activation of the mammalian target of rapamycin (mTOR) pathway in adiponectin-deficient (KO) mice compared with that in wild-type (WT) mice under the high-fat diet condition. Western blot analysis for phosphorylated and total AMP-activated protein kinase (AMPK) (A), mTOR (B), p70 S6 kinase (C) and S6 protein (D) in the colon from the WT and KO mice under the high-fat diet condition. Left panels: Pictures of the western blotting. Right panels: Graphs showing the ratios of the phosphorylated protein to the total protein. Each column represents the mean (with the SEM), *$p<0.05$.

activation of the mTOR pathway directly involved in cell proliferation. To confirm whether adiponectin actually suppresses the AMPK/mTOR pathway, we treated mice with the specific AMPK activator AICAR, or the mTOR inhibitor rapamycin. The increase of cell proliferation in the colon epithelium was significantly suppressed by AICAR in the KO mice under the high-fat diet, but no effect in WT mice under high-fat diet (fig 6A,B). Similarly, ACF formation was significantly suppressed by AICAR in the KO mice under the high-fat diet, but not in the WT mice (fig 6C). In the KO mice under the high-fat diet, treatment with rapamycin significantly reduced the BrdU index in a dose dependent manner and ACF formation (fig 6D,E). These results indicate that the activation of the mTOR pathway may play important roles in the increase in epithelial cell proliferation in KO mice under the high-fat diet, and may play an important role in the promotion of colon carcinogenesis in KO mice under the high-fat diet condition.

DISCUSSION

The existence of a relationship between high-fat diets and colorectal cancer has been speculated for a long time, but no definitive conclusions have been arrived at yet.[35] It has been reported that the secretion of adiponectin from adipocytes is suppressed in obese humans.[11] Considered together with the knowledge that obesity is also an important risk factor for colorectal cancer,[4] we speculated that adiponectin might suppress the development of colorectal cancer.

We demonstrated significantly enhanced formation of polyps and ACF in the KO mice compared with that in the WT mice under the high-fat diet. Furthermore, an increase in proliferative activity of colonic epithelial cells was also observed in the KO mice under the high-fat diet, but not under the basal diet. These results suggest that under the high-fat diet, but not under basal diet, a deficiency of adiponectin significantly promotes the proliferative activity of the colonic epithelial cells, and thereby may be promoting colorectal carcinogenesis. We demonstrated that the AdipoR1 is predominantly expressed in colon epithelium. The increase in the proliferative activity of the colonic epithelial cells and the number of ACF were observed in AdipoR1−/− mice, not in the AdipoR2−/− mice, under high-fat diet condition. These results suggest that the AdipoR1-mediated, but not the AdipoR2-mediated, pathway may play an important role in the suppressive effect of adiponectin on the increased in epithelial cell proliferation under the high-fat diet.

We demonstrated the activation of the mTOR pathway and inactivation of AMPK in colon epithelial cells in the KO mice under the high-fat diet, but there was no difference under the basal diet (data not shown). Moreover, the replacement of adiponectin ameliorated the activated mTOR pathway by adiponectin deficiency. AICAR, the AMPK specific activator, suppressed the increase in epithelial cell proliferation in KO mice, but not in WT littermates, under high-fat diet. Furthermore, rapamycin, an mTOR inhibitor, also significantly suppressed the increase in epithelial cell proliferation only in KO mice under high-fat diet in a dose dependent manner,

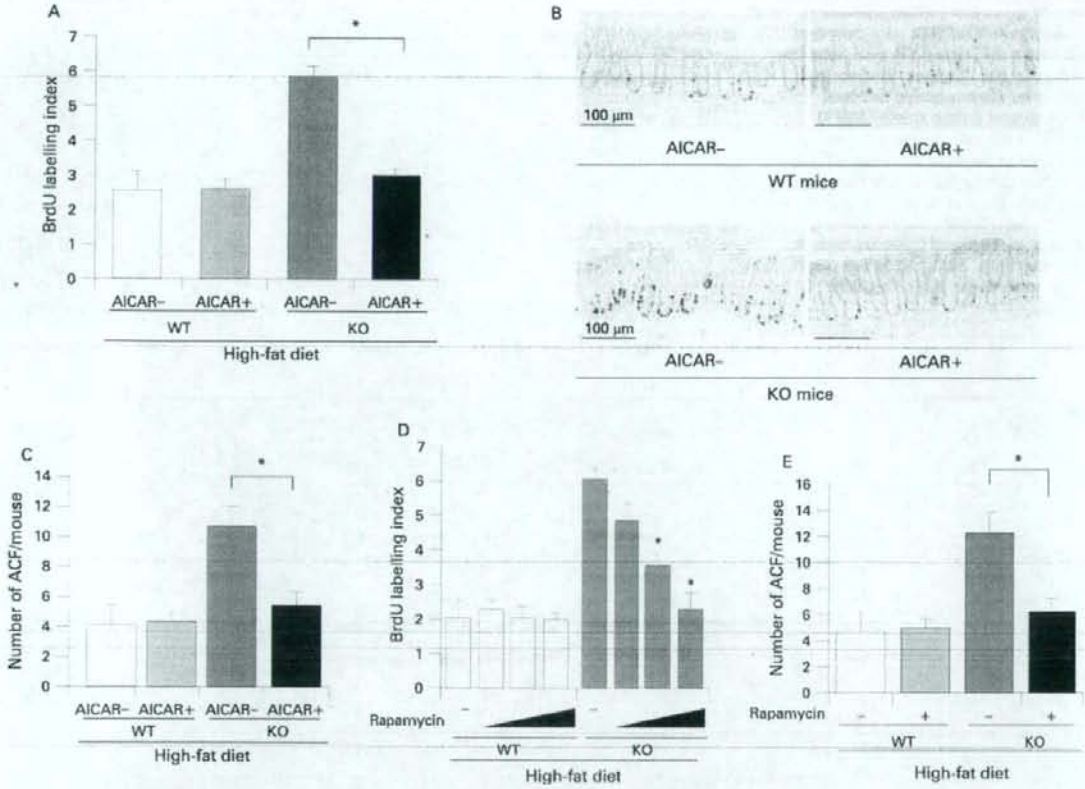

Figure 6 Suppression of epithelial cell hyper-proliferation by activation of AMP-activated protein kinase (AMPK) or by inhibition of the mammalian target of rapamycin (mTOR) in adiponectin-deficient (KO) mice under the high-fat diet condition. Wild-type (WT) mice (6 weeks old) were injected intraperitoneally with the AMPK activator 5-aminoimidazole-4-carboxamide-l-β-D-ribofuranoside (AICAR) (0.1 mg/kg/day), or vehicle until the end of the experiment. Mice in the high-fat diet group were also given two weekly intraperitoneal injections of 10 mg/kg of azoxymethane (AOM). (A) Average bromodeoxyuridine (BrdU) labelling index in the WT and KO mice treated (+) or not treated (−) with AICAR under the high fat diet condition. BrdU was administered intraperitoneally 1 h prior to the sacrifice of the animals. Each column represents the mean (with the SEM), *$p<0.05$. (B) Representative immunohistochemical staining patterns for BrdU in each group. (C) Average number of aberrant crypt foci (ACF) in the WT and KO mice treated (+) or not treated (−) with AICAR under the high fat diet condition. (D) WT and KO mice fed the high-fat (HF) diet were injected intraperitoneally with various doses of rapamycin (0.2, 0.4, 0.8 mg/kg) or only with vehicle every other day for 6 weeks. Average values of the BrdU index were decreased in the KO mice in a dose dependent manner, but not in the WT mice. *$p<0.05$ compared to non-treated KO mice. (E) Average number of ACF in the WT and KO mice treated (+) or not treated (−) with rapamycin (0.8 mg/kg) under the high fat diet condition. Each bar represents the mean (with the SEM), *$p<0.05$.

suggesting that mTOR plays an important role in promoting epithelial cell proliferation where there is a lack of adiponectin under a high-fat diet. It has been reported that AMPK directly inhibits mTOR.[28] Therefore we speculate that the AMPK/mTOR pathway is a possible mechanism closely involved in the protective effect of adiponectin in colon carcinogenesis under the high-fat diet (supplementary fig 7). Concerning other major pathways in the carcinogenesis, it was reported that adiponectin attenuated the adenomatous polyposis coli (APC)/β-catenin pathway,[36] and increased p53 expression[37] in different kinds of cancer cells. p53 also suppresses the mTOR pathway through activation of phosphatase and tensin homologue deleted on chromosome ten (PTEN), AMPK, insulin-like growth factor-1-binding protein 3 (IGF1-BP3) and tuberous sclerosis complex-2 (TSC-2).[38] Although the mechanism underlying the promotion of colon carcinogenesis by a high-fat diet is still unknown, our present data strongly suggest that plasma adiponectin derived from adipocytes suppresses the mTOR pathway through the activation of AMPK, resulting in suppression of the cell proliferative activity and, thereby, suppression of colon carcinogenesis, under the high-fat diet. However, in the event of a decrease in plasma adiponectin level, AMPK activity is suppressed, resulting in the activation of mTOR and the members downstream in the pathway, such as the p70 S6 kinase and S6 protein. We speculate that activation of the mTOR pathway directly promotes colonic epithelial cell proliferation and, thereby, colorectal carcinogenesis.

It has been reported that the plasma adiponectin levels are decreased in humans under the conditions of obesity and/or diabetes mellitus.[11] However, it was reported that plasma levels of adiponectin in the mice are not decreased in response to high-fat feeding for several weeks.[39] Therefore, we used

adiponectin-deficient mice to elucidate the role of adiponectin on colonic epithelial proliferation and carcinogenesis under the high-fat diet. Our experimental condition in which we used adiponectin-deficient mice fed a high-fat diet may well have reflected these pathophysiological conditions in humans.

The purpose of our study was to elucidate the role of adiponectin on colon carcinogenesis, not to elucidate the mechanism whereby a high-fat diet promotes carcinogenesis. This mechanism remains unknown. However, we could provide a possible mechanism underlying the protective roles of adiponectin in colorectal carcinogenesis promoted by a high-fat diet We consider that AMPK and mTOR may be novel therapeutic targets for the prevention of colorectal cancer under the low levels of plasma adiponectin in an obese population where the obesity is a result of a Western-style diet with a high fat content. Our results shed light on a novel mechanism by which adiponectin might suppress carcinogenesis mediated by a high-fat diet. Continued investigation to elucidate the precise mechanisms involved is necessary because of the major clinical implications.

Acknowledgements: We thank M Ochiai and M Hiraga for technical assistance.

Funding: This work was supported in part by a Grant-in-Aid for research on the Third Term Comprehensive Control Research for Cancer from the Ministry of Health, Labour and Welfare, Japan to AN; a grant from the National Institute of Biomedical Innovation (NBIO) to AN; a grant from the Ministry of Education, Culture, Sports, Science and Technology, Japan (KIBAN-B) to AN; and a research grant of the Princess Takamatsu Cancer Research Fund.

Competing interests: None.

Ethics approval: All animal experiments were approved by the institutional Animal Care and Use Committee of Yokohama City University School of Medicine.

REFERENCES

1. **Friedman JM.** Obesity in the new millennium. *Nature* 2000;**404**:632–4.
2. **Berg AH,** Combs TP, Schere PE. ACRP30/adiponectin: an adipokine regulating glucose and lipid metabolism. *Trends Endocrinol Metab* 2002;**13**:84–9.
3. **Shimomura I,** Funahashi T, Takahashi M, *et al.* Enhanced expression of PAI-1 in visceral fat: possible contributor to vascular disease in obesity. *Nature Med* 1996;**2**:800–3.
4. **Bianchini F,** Kaaks R, Vainio H. Overweight, obesity and cancer risk. *Lancet Oncol* 2002;**3**:565–74.
5. **Calle EE,** Rodriguez C, Walker-Thurmond K, *et al.* Overweight, obesity and mortality from cancer in a prospectively studied cohort of U.S. adults. *N Engl J Med* 2003;**348**:1625–38.
6. **Giovannucci E,** Goldin B. The role of fat, fatty acids, and total energy intake in the etiology of human colon cancer. *Am J Clin Nutr* 1997;**66**:1564S–71S.
7. **Reddy BS.** Dietary fat and colon cancer: animal model studies. *Lipids* 1992;**27**:807–13.
8. **Delporte ML,** El Mkadem SA, Quisquater M, *et al.* Leptin treatment markedly increased plasma adiponectin but barely decreased plasma resistin of *ob/ob* mice. *Am J Physiol Endocrinol Metab* 2004;**287**:E446–53.
9. **Yamauchi T,** Kamon J, Waki H, *et al.* The fat-derived hormone adiponectin reverses insulin resistance associated with both lipoatrophy and obesity. *Nature Med* 2001;**7**:941–46.
10. **Berg AH,** Combs TP, Du X, *et al.* The adipocyte-secreted protein Acrp30 enhances hepatic insulin action. *Nature Med* 2001;**7**:947–53.
11. **Arita Y,** Kihara S, Ouchi N, *et al.* Paradoxical decrease of an adipose-specific protein, adiponectin, in obesity. *Biochem Biophys Res Commun* 1999;**257**:79–83.
12. **Halleux CM,** Takahashi M, Delporte ML, *et al.* Secretion of adiponectin and regulation of apM1 gene expression in human visceral adipose tissue. *Biochem Biophys Res Commun* 2001;**288**:1102–7.
13. **Hotta K,** Funahashi T, Arita Y, *et al.* Plasma concentrations of a novel, adipose-specific protein, adiponectin, in type 2 diabetic patients. *Arterioscler Thromb Vasc Biol* 2000;**20**:1595–9.
14. **Giovannucci E,** Ascherio A, Rimm EB, *et al.* Physical activity, obesity, and risk for colon cancer and adenoma in men. *Ann Intern Med* 1995;**122**:327–34.
15. **Schoen RE,** Tangen CM, Kuller LH, *et al.* Increased blood glucose and insulin, body size, and incident colorectal cancer. *J Natl Cancer Inst* 1999;**91**:1147–54.
16. **Giovannucci E.** Insulin, insulin-like growth factors and colon cancer: a review of the evidence. *J Nutr* 2001;**131**:3109S–20S.
17. **Wei EK,** Giovannucci E, Fuchs CS, *et al.* Low plasma adiponectin levels and risk of colorectal cancer in men: a prospective study. *J Natl Cancer Inst* 2005;**97**:1688–94.
18. **Likanova A.** Serum adiponectin is not associated with risk of colorectal cancer. *Cancer Epidemiol Biomarkers Prev* 2006;**15**:401–2.
19. **Yamauchi T,** Kamon J, Ito Y, *et al.* Cloning of adiponectin receptors that mediate antidiabetic metabolic effects. *Nature* 2003;**423**:762–9.
20. **Yamauchi T,** Kamon J, Minokoshi Y, *et al.* Adiponectin stimulates glucose utilization and fatty-acid oxidation by activating AMP-activated protein kinase. *Nature Med* 2002;**8**:1288–95.
21. **Yamauchi T,** Nio Y, Maki T, *et al.* Targeted disruption of AdipoR1 and AdipoR2 causes abrogation of adiponectin binding and metabolic actions. *Nature Med* 2007;**13**:332–9.
22. **Averous J,** Proud CG. When translation meets transformation: the mTOR story. *Oncogene* 2006;**25**:6423–35.
23. **Guertin DA,** Sabatini DM. An expanding role for mTOR in cancer. *Trends Mol Med* 2005;**11**:353–61.
24. **Wullschleger S,** Loewith R, Hall MN. TOR signaling in growth and metabolism. *Cell* 2006;**124**:471–84.
25. **Avruch J,** Belham C, Weng Q, *et al.* The p70 S6 kinase integrates nutrient and growth signals to control translational capacity. *Prog Mol Subcell Biol* 2001;**26**:115–54.
26. **Sahin F,** Kannangai R, Adegbola O, *et al.* mTOR and p70 S6 kinase expression in primary liver neoplasms. *Clin Cancer Res* 2004;**10**:8421–5.
27. **Corradetti MN,** Guan KL. Upstream of the mammalian target of rapamycin: do all roads pass through mTOR? *Oncogene* 2006;**25**:6347–60.
28. **Luo Z,** Saha AK, Xiang X, *et al.* AMPK, the metabolic syndrome and cancer. *Trends Pharmacol Sci* 2005;**26**:69–76.
29. **Nakagama H,** Nakanishi N, Ochiai M. Modeling human colon cancer in rodents using a food-borne carcinogen, PhIP. *Cancer Sci* 2005;**96**:627–36.
30. **Osawa E,** Nakajima A, Wada K, *et al.* Peroxisome proliferator-activated receptor γ ligans suppress colon carcinogenesis induced by azoxymethane in mice. *Gastroenterology* 2003;**124**:361–7.
31. **McLellan EA,** Bird RP. Aberrant crypts: potential preneoplastic lesions in the murine colon. *Cancer Res* 1998;**48**:6187–92.
32. **Konstantakos AK,** Siu IM, Pretlow TG, *et al.* Human aberrant crypt foci with carcinoma in situ from a patient with sporadic colon cancer. *Gastroenterology* 1996;**111**:772–7.
33. **Nawrocki AR,** Rajala MW, Tomas E, *et al.* Mice lacking adiponectin show decreased hepatic insulin sensitivity and reduced responsiveness to peroxisome proliferator-activated receptor gamma agonists. *J Biol Chem* 2006;**281**:2654–60.
34. **Tomas E,** Tsao TS, Saha AK, *et al.* Enhanced muscle fat oxidation and glucose transport by ACRP30 globular domain: Acetyl-CoA carboxylase inhibition and AMP-activated protein kinase activation. *Proc Natl Acad Sci USA* 2002;**99**:16309–13.
35. **Zock PL.** Dietary fats and cancer. *Curr Opin Lipidol* 2001;**12**:5–10.
36. **Wang Y,** Lam JB, Lam KS, *et al.* Adiponectin modulates the glycogen synthase kinase-3beta/beta-catenin signaling pathway and attenuates mammary tumorigenesis of MDA-MB-231 cells in nude mice. *Cancer Res* 2006;**66**:11462–70.
37. **Mistry T,** Digby JE, Desai KM, *et al.* Leptin and adiponectin interact in the regulation of prostate cancer cell growth via modulation of p53 and bcl-2 expression. *Br J Urol Int* 2008;**101**:1317–22.
38. **Feng Z,** Hu W, Rajagopal G, *et al.* The tumor suppressor p53: cancer and aging. *Cell Cycle* 2008;**7**:842–7.
39. **Bullen JW Jr,** Bluher S, Kelesidis T, *et al.* Regulation of adiponectin and its receptors in response to development of diet-induced obesity in mice. *Am J Physiol Endocrinol Metab* 2007;**292**:E1079–86.

β-catenin is strongly elevated in rat colonic epithelium following short-term intermittent treatment with 2-amino-1-methyl-6-phenylimidazo[4,5-*b*]pyridine (PhIP) and a high-fat diet

Rong Wang,[1] W. Mohaiza Dashwood,[1] Christiane V. Löhr,[2] Kay A. Fischer,[2] Hitoshi Nakagama,[3] David E. Williams[1,4] and Roderick H. Dashwood[1,4,5]

[1]Linus Pauling Institute, [2]College of Veterinary Medicine, Oregon State University, Corvallis OR 97331-6512; [3]Biochemistry Division, National Cancer Center Research Institute, 1-1, Tsukiji 5-chome, Chuo-ku, Tokyo 104-0045, Japan; [4]Department of Environmental and Molecular Toxicology, Oregon State University, Corvallis OR 97331-6512, USA

(Received April 2, 2008/Revised April 24, 2008; May 13, 2008/Accepted May 13, 2008/Online publication July 4, 2008)

Colon tumors expressing high levels of β-catenin and c-myc have been reported in male F344 rats given three short cycles of 2-amino-1-methyl-6-phenylimidazo[4,5-*b*]pyridine (PhIP) alternating with a high-fat (HF) diet. Using the same experimental protocol, rats were euthanized 24 h after the last dose of PhIP so as to examine early changes in colonic crypt homeostasis and β-catenin expression, before the onset of frank tumors. PhIP/HF dosing caused a significant increase in the bromodeoxyuridine labeling index throughout the entire colon, and within the colonic crypt column cleaved caspase-3 was elevated in the basal and central zones, but reduced in the luminal region. In vehicle/HF controls, β-catenin was immunolocalized primarily at the border between cells at the top of the crypt, whereas in rats given PhIP/HF diet there was strong cytoplasmic staining, which appeared as a gradient of increased β-catenin extending from the base of the crypt column to the luminal region. Quantitative real-time PCR and immunoblot analyses confirmed that β-catenin and c-myc were increased significantly in the colonic mucosa of rats given PhIP/HF diet. Collectively, these findings suggest that PhIP/HF cycling alters β-catenin and c-myc expression in the colonic mucosa, resulting in expansion of the proliferative zone and redistribution of apoptotic cells from the lumen to the central and basal regions of the colonic crypt. Thus, during the early stages of colon carcinogenesis, alternating exposure to heterocyclic amines and a high-fat diet might facilitate molecular changes resulting in dysregulated β-catenin and c-myc expression. (*Cancer Sci* 2008; 99: 1754–1759)

High-temperature cooking of meat and fish generates heterocyclic amine mutagens,[1] including the compound 2-amino-1-methyl-6-phenylimidazo[4,5-*b*]pyridine (PhIP).[2] PhIP is a multiorgan carcinogen in the rat, inducing tumors of the colon, prostate, mammary gland and other sites.[3] These tumors are characterized by high expression levels of β-catenin and β-catenin/T-cell factor (Tcf) target genes,[4–7] as seen in primary human colon cancers and human colorectal cancer cell lines.[8–10]

Recently, it was reported that three short cycles of PhIP alternating with a high-fat (HF) diet was as effective for the induction of colon tumors as continuous dietary treatment with the carcinogen.[11,12] It was speculated that with continuous PhIP administration, multiple disadvantageous mutations might interfere with the growth of focal populations, resulting in cell death, so that only a subset of transformed cells survive and proliferate. It was suggested that intervals between PhIP exposure might produce 'less chance of lethal mutations occurring [and] high-fat diet could directly promote cell growth'.[11] This selection process might be further influenced by postinitiation exposure to dietary phytochemicals, so that certain oncogenic mutants progress in preference to others, such as those affecting β-catenin stability.[7,12]

To provide insight into the possible selection pressures during early stages of colon carcinogenesis, we examined the effects of short-term intermittent PhIP/HF diet exposure on colonic cell homeostasis in the rat, before the onset of frank colon tumors. We report here on the induction of cell proliferation and apoptosis within the proliferative zone of the colonic crypt, with strongly elevated levels of cytoplasmic and nuclear β-catenin. There was a concomitant increase in β-catenin and c-myc mRNA and protein expression, consistent with results obtained in colon tumors at 1 year.[12]

Materials and Methods

Animals and treatment. Prior approval was obtained from the Institutional Animal Care and Use Committee. The treatment protocol is illustrated in Fig. 1, and full details were reported recently by Wang *et al.*[12] In brief, male F344 rats obtained at 4–5 weeks of age from the US National Cancer Institute were housed two per cage and given AIN93G diet (Dyets Inc., Bethlehem, PA) and water *ad libitum*. After 1 week acclimatization to the cages, PhIP (Toronto Research Chemicals, Ontario, Canada) was administered to each rat by daily oral gavage at a dose of 50 mg/kg body weight, which approximates the daily exposure in rats given 400 parts per million (p.p.m.) PhIP in the diet.[13] Controls received vehicle alone (0.8% dimethyl sulfoxide [DMSO] in ultra-pure water, adjusted to pH 3.5 with 0.1 N HCl). Following 2 weeks of PhIP or vehicle treatment, rats were placed on AIN93G diet supplemented with Primex hydrogenated vegetable oil, comprising 23% fat-derived calories, and referred to hereafter as high-fat (HF) diet. This diet was obtained from a commercial vendor (Dyets Inc., Bethlehem, PA, USA), and the composition is shown in Table 1. After 4 weeks on HF diet, animals were returned to standard AIN93G diet and treated again with PhIP or vehicle for 2 weeks, followed by an additional 4 weeks on HF diet. A third cycle of PhIP or vehicle then was completed, and 24 h later the rats were euthanized by CO_2 inhalation. Colons from four

[5]To whom correspondence should be addressed.
E-mail: Rod.Dashwood@oregonstate.edu

doi: 10.1111/j.1349-7006.2008.00887.x

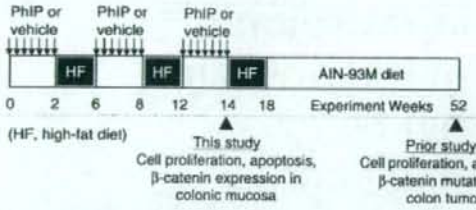

Fig. 1. Experimental protocol for short-term intermittent 2-amino-1-methyl-6-phenylimidazo[4,5-*b*]pyridine (PhIP) treatment alternating with high-fat diet. This figure was modified from a recent report by Wang *et al.*, which provided full details of the treatment protocol.[12] In brief, male F344 rats were given PhIP by daily oral gavage at a dose of 50 mg/kg body weight, whereas controls received vehicle alone (0.8% dimethyl sulfoxide [DMSO] in ultra-pure water, adjusted to pH 3.5 with 0.1 N HCl). Following 2 weeks of PhIP or vehicle treatment, rats were placed on AIN93G diet supplemented with Primex hydrogenated vegetable oil, comprising 23% fat-derived calories (high-fat [HF] diet). After 4 weeks on HF diet, animals were returned to standard AIN93G diet and treated again with PhIP or vehicle for 2 weeks, followed by an additional 4 weeks on HF diet. A third cycle of PhIP or vehicle then was completed, and 24 h later the rats were euthanized by CO_2 inhalation. Note: in our prior study, which lasted 1 year,[12] rats were switched as recommended from AIN93G (growth) diet to AIN94M (maintenance) diet at week 18.

PhIP-treated rats and three vehicle-treated rats were Swiss-rolled and fixed in 10% formalin for immunohistochemical analyses. Colons from five additional PhIP-treated rats and six vehicle-treated rats were opened longitudinally, and the mucosa was scraped and frozen in liquid nitrogen, then stored at –80°C for subsequent molecular work.

Scoring of cell proliferation and apoptosis indices. Details of the methods used for tissue isolation and immunohistochemistry were reported elsewhere.[12] In brief, 5–6 rats in each group were selected at random and injected *i.p.* with bromodeoxyuridine (BrdU, 200 μmol/kg body wt), 1 h before sacrifice. Colons were removed and processed for immunostaining using the BrdU *in situ* detection kit (BDBiosciences, San Jose, CA, USA). In addition, cleaved caspase-3 was immunolocalized using the EnVision+System-HRP Kit (Dako, Carpinteria, CA, USA) in conjunction with a polyclonal rabbit anticleaved caspase-3 antibody, which detects the endogenous large fragment of cleaved caspase-3 resulting from cleavage adjacent to Asp175 (Cell Signaling Inc., Danvers, MA, USA). Labeling indices were calculated as the number of positive cells divided by the total number of cells in the basal, central and apical regions of the colonic crypt column, for a minimum of 15 crypts in each of the distal, middle and proximal regions of the colon (=45 crypts scored per colon). Only complete, well-oriented, longitudinally sectioned crypts were evaluated.

Immunohistochemical detection of β-catenin. The basic method was identical to that used for cleaved caspase-3, but with polyclonal rabbit antiβ-catenin (Abcam, ab2982, Cambridge, MA, USA) at 500-fold dilution in phosphate-buffered saline.

Quantitative real-time PCR (qPCR). *Ctnnb1* (β-catenin), *cyclin D1*, c-*myc* and c-*jun* mRNA levels were determined by quantitative (q)PCR and normalized to glyceraldehyde-3-phosphate dehydrogenase (*Gapdh*), exactly as reported.[5,12] In brief, frozen samples of colonic mucosa (5–6 rats per group) were thawed and the mRNA was extracted using the RNeasy kit (Qiagen, Valencia, CA, USA). RNA was reverse-transcribed using Omniscript Reverse Transcriptase (Qiagen) and random hexamers (Invitrogen). PCR was conducted on an Opticon Monitor 2 system (Finnzymes, Finland), in 20 μL total reaction volume containing cDNAs, SYBR Green I dye (DyNAmo master solution, Finnzymes) and gene-specific primers. The amount of specific mRNA was quantified by determining the point at which the fluorescence accumulation entered the exponential phase (C_t), and the C_t ratio of the target gene to *Gapdh* was calculated for each sample. Three separate experiments were performed for each sample, and the corresponding results were expressed as mean ± SE.

Immunoblotting. β-Catenin, c-myc, c-jun and cyclin D1 were examined using the immunoblotting methodology reported elsewhere, with β-actin as loading control.[6,7]

Statistics. Data were plotted as mean ± SE and compared using Students *t*-test. In the figures, significant *P*-values are shown as follows: $*P < 0.05$, $**P < 0.01$, $***P < 0.001$.

Results

Cycling of PhIP/HF diet strongly induces cell proliferation throughout the colon. Immunohistochemical staining for BrdU incorporation revealed a marked difference between vehicle- and PhIP-treated rats (Fig. 2). When quantified for the entire crypt column (Fig. 2a), the BrdU labeling index showed a highly significant increase in rats given PhIP in the proximal, middle and distal regions of the colon. Specifically, 6–9% of the cells were BrdU-positive in vehicle controls, compared with 14–19% in rats given PhIP. BrdU-positive cells also were quantified for different regions within the crypt column (Fig. 2b–d); increased labeling was seen in the central and basal regions, with little or no change in the luminal zone (upper-third).

Cycling of PhIP/HF diet alters the distribution of apoptotic cells within the colonic crypt. Immunohistochemical staining for cleaved caspase-3, a marker of apoptosis, identified positive cells along the uppermost region of the crypt in vehicle controls, and more generalized staining throughout the crypt column in rats given PhIP (Fig. 3). Quantification of the labeling index for the entire crypt column showed no significant differences in the proximal, middle or distal regions of the colon (Fig. 3a). However, when

Table 1. Composition of AIN93G and high-fat (HF) AIN93G diets

Ingredient	AIN93G (Dyets #110700) g/kg	HF AIN93G (Dyets #181059) g/kg
Casein	200	200
L-Cystine	3	3
Sucrose	100	63.5
Cornstarch	397.486	252.186
Dyetrose	132	83.8
Soybean oil	70	70
t-Butylhydroquinone	0.014	0.014
Primex (hydrogenated vegetable oil)	0	230
Cellulose	50	50
Mineral mix #210025	35	35
Vitamin mix #310025	10	10
Choline bitartrate	2.5	2.5
Total	1000	1000

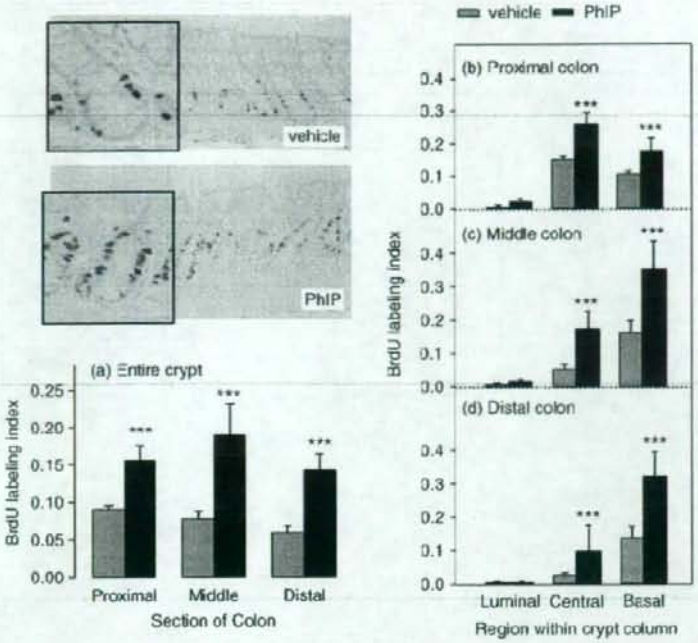

Fig. 2. Cycling of 2-amino-1-methyl-6-phenylimidazo[4,5-*b*]pyridine (PhIP)/high-fat diet induces cell proliferation in the colon. Rats were treated with PhIP and a high-fat diet (see Fig. 1) and the bromodeoxyuridine (BrdU) labeling index was determined as described in Materials and Methods. Data bars, mean ± SE; ***$P < 0.001$, by Students *t*-test, PhIP ($n = 4$) *versus* corresponding vehicle controls ($n = 3$).

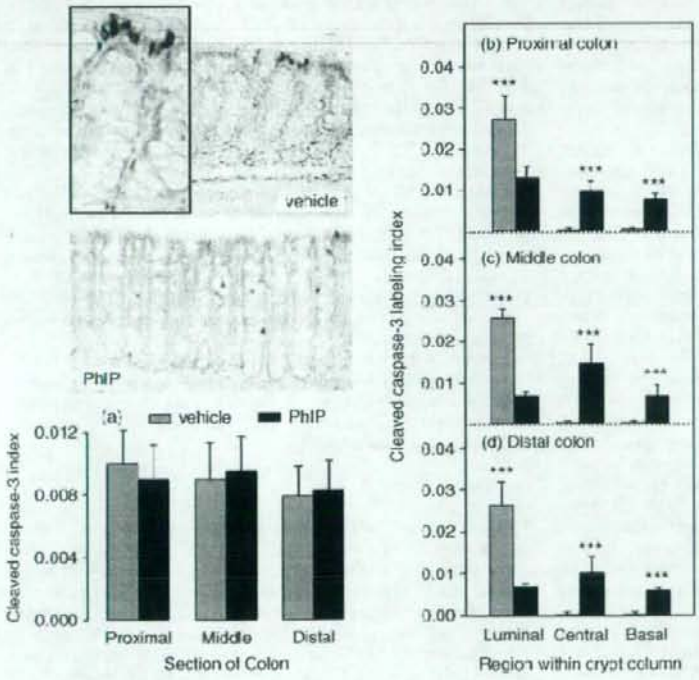

Fig. 3. Cycling of 2-amino-1-methyl-6-phenylimidazo[4,5-*b*]pyridine (PhIP)/high-fat diet increases cleaved caspase-3 labeling in the central and basal regions of the colonic crypt column and reduces it in the luminal region. The cleaved caspase-3 labeling index was determined as described in Materials and Methods. Data bars, mean ± SE; ***$P < 0.001$, by Students *t*-test, PhIP ($n = 4$) *versus* corresponding vehicle controls ($n = 3$).

doi: 10.1111/j.1349-7006.2008.00887.x

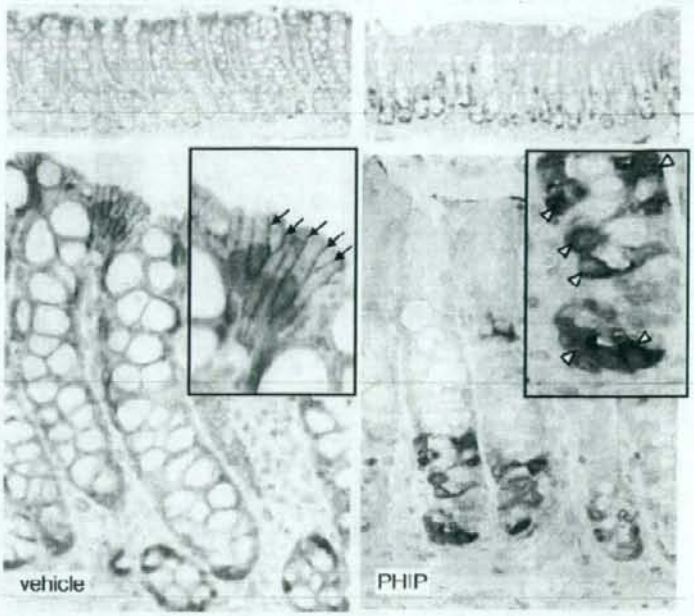

Fig. 4. Cycling of 2-amino-1-methyl-6-phenylimidazo[4,5-*b*]pyridine (PhIP)/high-fat diet increases β-catenin expression in the colon. Immunohistochemistry revealed low overall expression levels of β-catenin in vehicle controls, but high levels in PhIP-treated rats. In vehicle controls, β-catenin was restricted to the borders between cells (arrows), with little or no cytoplasmic and nuclear staining, whereas in PhIP-treated rats there was strong cytoplasmic β-catenin expression (arrow heads).

the cleaved caspase-3 labeling index was quantified for regions within the crypt column (Fig. 3b–d), a highly significant difference was seen between vehicle controls and PhIP-treated rats. In the latter case, cleaved caspase-3-positive cells were more-or-less evenly distributed throughout the luminal, central and basal crypt regions, whereas in vehicle controls the labeling was almost exclusively in the luminal region of the crypt. We interpret these data as evidence that PhIP/HF cycling increased cell proliferation in the lower two-thirds of the crypt (Fig. 2), giving rise to more apoptotic cells in the same region and a concomitant reduction in cell death at the top of the crypt.

Cycling of PhIP/HF diet increases β-catenin staining in the colonic crypt. An important regulator of cell proliferation and apoptosis in the colon is β-catenin and immunohistochemical staining revealed a marked difference in β-catenin expression within the crypt column of rats given PhIP compared with vehicle (Fig. 4). Thus, in vehicle controls, histological studies showed there was a generalized low level of β-catenin expression that was restricted to the borders between cells in the upper region of the crypt column (arrows), with no cytoplasmic or nuclear staining detected. In marked contrast, colons from rats given PhIP had widespread labeling throughout the lower half to two-thirds of the crypt column and β-catenin was strongly expressed in the cytoplasm and sometimes also in the nucleus (Fig. 4, open arrowheads).

Quantification of β-catenin-positive cells revealed significant differences between vehicle- and PhIP-treated rats. Specifically, in vehicle controls, <0.2% of the cells stained positive for nuclear and/or cytoplasmic β-catenin (grey bars, Fig. 5a), but ~78% of the cells were positive for membrane-associated β-catenin (grey bars, Fig. 5b), and this was seen in the proximal, middle and distal regions of the colon. In the proximal colon of PhIP-treated rats, 4% of the cells stained positive for nuclear/cytoplasmic β-catenin (solid bar, Fig. 5a) and ~25% for membrane-associated β-catenin (solid bar, Fig. 5b). In the middle colon, the corresponding data were 8–9% for nuclear/cytoplasmic β-catenin and 18.5% for membrane-associated β-catenin. In the distal colon of both PhIP- and vehicle-treated rats, ~75% of the cells stained positive for membrane-associated β-catenin (Fig. 5b), but few cells had nuclear/cytoplasmic staining.

Nuclear/cytoplasmic β-catenin labeling was further examined according to region within the colonic crypt column (Fig. 5c). There was evidence for a gradient of increased β-catenin expression in the colonic crypt of PhIP-treated rats compared with vehicle controls, with higher β-catenin levels in the basal zone than in the central or luminal zones. The data presented in Fig. 5(c) for PhIP-treated rats (solid bars) revealed 2%, 5.6% and 17.2% of the cells stained positive for nuclear/cytoplasmic β-catenin in the luminal, central and basal regions of the crypt, respectively ($P < 0.001$, each region *versus* the corresponding vehicle control).

Cycling of PhIP/HF diet elevates β-catenin and c-myc mRNA and protein expression. We next examined *Ctnnb1* (β-catenin) and three β-catenin/Tcf target genes, c-*myc*, c-*jun* and *cyclin D1*, for changes in mRNA expression (Fig. 6). Colonic mucosa from PhIP-treated rats had 30% higher levels of *Ctnnb1* and 65% higher levels of c-*myc* mRNA compared with vehicle controls ($P < 0.05$). No difference in c-*jun* or *cyclin D1* expression was observed after normalizing to *Gapdh*.

Immunoblotting revealed higher expression levels of β-catenin and c-myc proteins in colonic mucosa of PhIP-treated rats, compared with vehicle controls (Fig. 7). No differences were seen among the treatment groups for cyclin D1 and c-jun, after normalizing to β-actin (data not shown).

Discussion

Ubagai *et al.* studied the combined effects of PhIP and a HF diet on colon carcinogenesis in the F344 rat.[11] Animals were given 400 p.p.m. PhIP in the basal diet for 2 weeks, followed by HF diet for up to 110 weeks, and this resulted in 3 of 19 rats with large intestinal tumors (19% incidence). Alternatively, 400 p.p.m. dietary PhIP was given for 2 weeks, followed by 4 weeks on HF diet, and the PhIP/HF cycling was repeated three times, ending with continuous HF diet for up to 60 weeks. Large

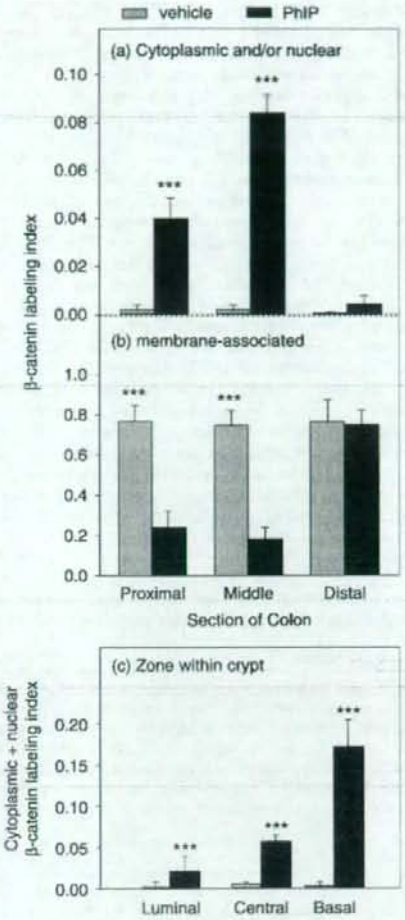

Fig. 5. Cycling of 2-amino-1-methyl-6-phenylimidazo[4,5-*b*]pyridine (PhIP)/high-fat diet increases cytoplasmic β-catenin expression in the colon. The β-catenin labeling index was scored as the number of cells stained positively for cytoplasmic (and/or nuclear) *versus* membrane-associated expression, divided by the total number of cells in that region of the colon. Data bars, mean ± SE; PhIP $n = 4$, vehicle controls $n = 3$. $^{**}P < 0.01$; $^{***}P < 0.001$, PhIP group significantly different from the corresponding vehicle controls.

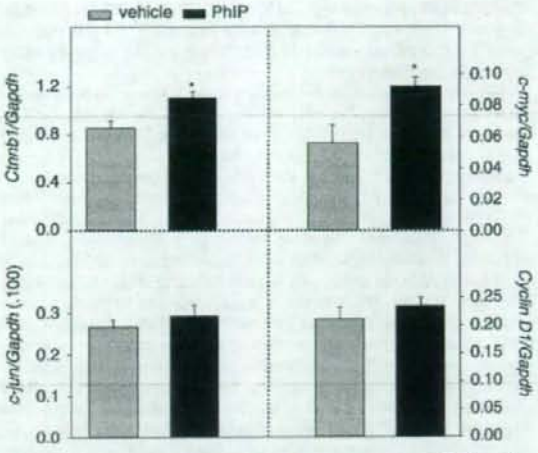

Fig. 6. Cycling of 2-amino-1-methyl-6-phenylimidazo[4,5-*b*]pyridine (PhIP)/HF diet increases β-catenin and c-myc mRNA expression in the rat colon. Quantitative real-time PCR was performed as described in Materials and Methods, for β-catenin (*Ctnnb1*) and three β-catenin/Tcf target genes, namely *c-myc*, *c-jun* and *cyclin D1*, normalized to *Gapdh*. Data bars, mean ± SE, PhIP $n = 5$, vehicle controls $n = 6$. $^{*}P < 0.05$, PhIP group significantly different from corresponding vehicle controls.

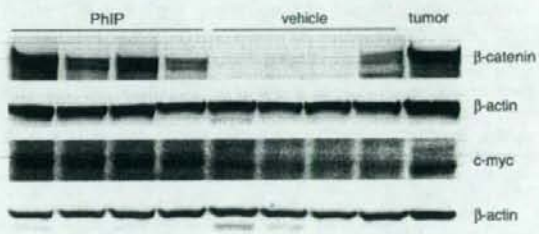

Fig. 7. Immunodetection of increased β-catenin and c-myc in the rat colon before the onset of frank tumors. Representative immunoblots of β-catenin and c-myc in colonic mucosa from rats treated with three cycles of 2-amino-1-methyl-6-phenylimidazo[4,5-*b*]pyridine (PhIP) (or vehicle) alternating with high-fat diet. A PhIP-induced colon tumor from the corresponding 1-year carcinogenicity study,[12] is shown in the furthest right lane as a positive control. β-Actin, loading control.

intestinal tumors were seen in 9 out of 20 rats (45% incidence). The latter result compares favorably with the 43% incidence observed in rats treated continuously with 100 p.p.m. dietary PhIP for 104 weeks,[3] in which a ~10-fold greater total amount of PhIP was administered per animal. Thus, PhIP/HF cycling represents an efficient means of inducing colon tumors, using a fraction of the amount of total carcinogen. We further modified the experimental protocol by giving PhIP via oral gavage, at a dose (50 mg/kg body wt per day) that was matched to the daily carcinogen intake from 400 p.p.m. PhIP in the diet,[3] and after three cycles of PhIP/HF treatment, standard AIN93M diet rather than HF diet was administered. Using this modified protocol, the colon tumor incidence after 1 year was 41.6%.[12]

In the current investigation, rats were euthanized immediately after completing the third and final cycle of PhIP dosing, so as to examine changes in colonic crypt homeostasis before the onset of frank tumors. Under these conditions, there was a striking increase in BrdU-positive cells throughout the entire length of the colon, with particularly high staining in the lower two-thirds of the crypt column. Moreover, there was an increase in cleaved caspase-3-positive cells in the proliferative zone of each crypt (central and basal regions), coupled with a reduction of apoptotic cells in the luminal region. The present study was not designed to specifically compare intermittent PhIP/HF dosing with continuous dietary PhIP treatment, but this might be interesting in a follow up investigation. Previously, a modest 1.5-fold increase in colonic BrdU labeling was seen at 8 weeks in male (but not female) rats fed continuously with 400 p.p.m. PhIP in the diet, and no significant changes were seen in cell proliferation rates for male or female rats at 4 or 12 weeks.[13] However, the latter

doi: 10.1111/j.1349-7006.2008.00887.x

study did not assess changes in apoptosis or β-catenin expression. In general, we observed that cleaved caspase-3 did not show as good a concordance as did BrdU labeling for the corresponding β-catenin positive cells.

The high cytoplasmic β-catenin expression seen in the present study is noteworthy, because Ubagai *et al.*[11] reported that all of the large intestinal tumors obtained following PhIP/HF treatment also had high accumulation of cytoplasmic and nuclear β-catenin. Interestingly, only 55% of the tumors harbored a mutation in the *Apc* or *Ctnnb1* (β-catenin) genes, and it was suggested that PhIP/HF cycling produced 'unknown genetic alterations' in the Wnt–Apc–β-catenin signaling pathway.[11] Using the identical exposure protocol described here, colon tumors obtained at 1 year had a 36% frequency of β-catenin mutations, although this was increased to 79% when rats were subjected to postinitiation treatment with caffeine, which resulted in tumor promotion.[12] This clearly supports the notion that cells harboring specific genetic changes within a population can be influenced to progress (or not to progress) to neoplasia by external factors, such as phytochemicals and a HF diet. As discussed before,[11] intermittent exposure to PhIP might allow populations of cells to survive and progress to tumors, when continuous carcinogen treatment might otherwise lead to removal of those cells via apoptosis. In the present study, there was increased apoptosis in the lower half of the colonic crypt following PhIP cycling, but this appeared to be a compensatory mechanism triggered by the greatly enhanced rate of cell proliferation, resulting in expansion of the crypt-wide proliferative zone (Fig. 2).

Despite the high levels of β-catenin detected in the present study following PhIP/HF treatment (Fig. 4), no β-catenin mutations were observed in the colonic mucosa scrapings, using PCR-based single strand conformation polymorphism (PCR-SSCP) screening (data not presented). One interpretation is that β-catenin mutations were indeed present in the colonic scrapings, but below the limit of detection of the PCR-SSCP methodology, and that only after clonal expansion and tumor formation were the mutations readily detected owing to their enrichment relative to the wild type allele. Interestingly, among the three reported β-catenin/Tcf target genes examined, only c-*myc* was increased in the colonic mucosa of rats given PhIP/HF diet, as noted in the colon tumors obtained at 1 year.[12] Interestingly, *Ctnnb1* mRNA also was elevated in the colonic mucosa of rats given PhIP/HF diet (Fig. 6). Although this increase was modest, it is consistent with prior reports showing elevated levels of *Ctnnb1* mRNA expression in PhIP- and 1,2-dimethylhydrazine-induced rat colon tumors,[5,12] as well as in primary human colon carcinomas and their liver metastases.[14] In some of the vehicle controls, low or undetectable levels of β-catenin were seen via immunoblotting (Fig. 7), despite the presence of *Ctnnb1* mRNA in most samples (Fig. 6) and membrane-associated β-catenin being detected in immunohistochemical analyses (Fig. 4). It is unclear whether this reflects the efficiency of the membrane extraction and/or immunoblot procedures used here, and further work is needed to clarify this question, perhaps on a larger subset of tissue samples from vehicle and PhIP-treated animals. However, for the vehicle control samples shown here (Fig. 7), repeated immunoblotting confirmed the low or undetectable expression of β-catenin, suggesting the data in this case were reproducible.

In summary, we have shown that in rats given three cycles of PhIP alternating with exposure to HF diet, there was an increase in colonic cell proliferation, elevated apoptosis in the proliferative zone of the colonic crypt and augmented expression of cytoplasmic β-catenin. These results from the early stages of colon carcinogenesis suggested a possible independent dysregulation of β-catenin and c-myc expression, separate from the classical β-catenin/Tcf pathway,[15] in accordance with data obtained from the corresponding colon tumors at 1 year.[12] Thus, early changes affecting colonic crypt homeostasis at the time of exposure to PhIP and HF diet may have persisted into much later stages of colon tumor formation.

Acknowledgments

We thank Mandy Louderback for assistance with oral gavage and necropsy. Laboratory Animal Service (LAR) staff are gratefully acknowledged for their help with animal care and maintenance. The experiments described here were supported in part by NIH grants CA90890, CA65525, CA90176 and CA122959, and by National Institute of Environmental Health Sciences Center grant P30 ES00210. Partial support for RHD was provided by the Foundation for Promotion of Cancer Research, Tokyo, Japan.

References

1 Sugimura T, Wakabayashi K, Nakagama H, Nagao M. Heterocyclic amines: mutagens/carcinogens produced during cooking of meat and fish. *Cancer Sci* 2004; **95**: 290–9.
2 Knize MG, Felton JS. Formation and human risk of carcinogenic heterocyclic amines formed from natural precursors in meat. *Nutr Rev* 2005; **63**: 158–65.
3 Ito N, Hasegawa R, Imaida K *et al.* Carcinogenicity of 2-amino-1-methyl-6-phenylimidazo[4,5-*b*]pyridine (PhIP) in the rat. *Mutat Res* 1997; **376**: 107–14.
4 Dashwood RH, Suzui M, Nakagama H, Sugimura T, Nagao M. High frequency of β-catenin (*Ctnnb1*) mutations in the colon tumors induced by two heterocyclic amines in the F344 rat. *Cancer Res* 1998; **58**: 1127–9.
5 Wang R, Dashwood WM, Bailey GS, Williams DE, Dashwood RH. Tumors from rats given 1,2-dimethylhydrazine plus chlorophyllin or indole-3-carbinol contain transcriptional changes in β-catenin that are independent of β-catenin mutation status. *Mutat Res* 2006; **601**: 11–18.
6 Blum CA, Tanaka T, Zhong X *et al.* Mutational analysis of *Ctnnb1* and *Apc* in tumors from rats given 1,2-dimethylhydrazine or 2-amino-3-methylimidazo[4,5-*f*]quinoline: mutational 'hotspots' and the relative expression of β-catenin and c-jun. *Mol Carcinogen* 2003; **36**: 195–203.
7 Blum CA, Xu M, Orner GA *et al.* β-Catenin mutation in rat colon tumors initiated with 1,2-dimethylhydrazine and 2-amino-3-methylimidazo[4,5-*f*]quinoline, and the effect of post-initiation treatment with chlorophyllin and indole-3-carbinol. *Carcinogenesis* 2001; **22**: 315–20.
8 Segditsas S, Tomlinson I. Colorectal cancer and genetic alterations in the Wnt pathway. *Oncogene* 2006; **25**: 7531–7.
9 Gavert N, Ben-Ze'ev A. beta-Catenin signaling in biological control and cancer. *J Cell Biochem* 2007; **102**: 820–8.
10 Wood LD, Parsons DW, Jones S *et al.* The genomic landscapes of human breast and colorectal cancers. *Science* 2007; **318**: 1108–13.
11 Ubagai T, Ochiai M, Kawamori T *et al.* Efficient induction of rat large intestinal tumors with a new spectrum of mutations by intermittent administration of 2-amino-1-methyl-6-phenylimidazo[4,5-*b*]pyridine in combination with a high-fat diet. *Carcinogenesis* 2002; **23**: 197–200.
12 Wang R, Dashwood WM, Löhr CV *et al.* Protective versus promotional effects of white tea and caffeine on PhIP-induced tumorigenesis and β-catenin expression in the rat. *Carcinogenesis* 2008; **29**: 834–9.
13 Ochiai M, Watanabe M, Kushida H, Wakabayashi K, Sugimura T, Nagao M. DNA adduct formation, cell proliferation, and aberrant crypt focus formation induced by PhIP in male and female rat colon with relevance to carcinogenesis. *Carcinogenesis* 1996; **17**: 95–8.
14 Mann B, Gelos M, Siedow A *et al.* Target genes of β-catenin-T cell-factor/lymphoid-enhancer-factor signaling in human colorectal carcinomas. *Proc Natl Acad Sci USA* 1999; **96**: 1603–8.
15 Yekkala K, Baudino TA. Inhibition of intestinal polyposis with reduced angiogenesis in ApcMin/+ mice due to decreases in c-Myc expression. *Mol Cancer Res* 2007; **5**: 1296–303.

OPEN ACCESS Freely available online

PLoS one

The Anti-Proliferative Effects of the CHFR Depend on the Forkhead Associated Domain, but not E3 Ligase Activity Mediated by Ring Finger Domain

Tomokazu Fukuda, Yasuyuki Kondo, Hitoshi Nakagama*

Biochemistry Division, National Cancer Center Research Institute, Tokyo, Japan

Abstract

The CHFR protein comprises fork head associated- (FHA) and RING-finger (RF) domain and is frequently downregulated in human colon and gastric cancers up to 50%. The loss of CHFR mRNA expression is a consequence of promoter methylation, suggesting a tumor suppressor role for this gene in gastrointestinal carcinogenesis. In terms of the biological functions of CHFR, it has been shown to activate cell cycle checkpoint when cells are treated with microtubule depolymerizing agents. Furthermore, CHFR was reported to have E3 ligase activity and promote ubiquitination and degradation of oncogenic proteins such as Aurora A and polo-like kinase 1. However, molecular pathways involved in the tumor suppressive function of CHFR are not yet clear since the two established roles of this protein are likely to inhibit cell growth. In this study, we have identified that the FHA domain of CHFR protein is critical for growth suppressive properties, whereas the RF and cysteine rich domains (Cys) are not required for this function. In contrast, the RF and Cys domains are essential for E3 ligase activity of CHFR. By the use of a cell cycle checkpoint assay, we also confirmed that the FHA domain of CHFR plays an important role in initiating a cell cycle arrest at G2/M, indicating a functional link exists between the anti-proliferative effects and checkpoint function of this tumor suppressor protein via this domain. Collectively, our data show that the checkpoint function of the FHA domain of CHFR is a core component of anti-proliferative properties against the gastrointestinal carcinogenesis.

Citation: Fukuda T, Kondo Y, Nakagama H (2008) The Anti-Proliferative Effects of the CHFR Depend on the Forkhead Associated Domain, but not E3 Ligase Activity Mediated by Ring Finger Domain. PLoS ONE 3(3): e1776. doi:10.1371/journal.pone.0001776

Editor: Edathara Abraham, University of Arkansas, United States of America

Received January 28, 2008; **Accepted** February 12, 2008; **Published** March 12, 2008

Funding: This work was supported in part by a Grant-in-Aid for Cancer Research for the Third-Term Comprehensive 10-Year Strategy for Cancer Control from the Ministry of Health, Labour and Welfare of Japan, and by a Research Grant of the Sankyo Foundation of Life Science (06-016). Y.K. is a recipient of a Research Resident Fellowship from the Foundation for the Promotion of Cancer Research in Japan.

Competing Interests: The authors have declared that no competing interests exist.

* E-mail: hnakagam@gan2.res.ncc.go.jp

Introduction

CHFR (Checkpoint protein with Forkhead associated and Ring finger domain) was first isolated by a homology screening of EST cDNA clones harboring an FHA domain [1]. The CHFR protein is characterized by the existence of two domain structures that are well conserved across different species, namely the FHA and RING finger domains (RF) [1]. CHFR is in fact the only protein in vertebrates that contains both of these functional domains.

The FHA domain of CHFR has been reported to arrest the cell cycle under mitotic stress conditions caused by microtubule depolymerizing agents such as nocodazole, and this moiety thus confers a mitotic checkpoint function upon this protein [2–6]. In terms of the mechanisms underlying this checkpoint function, CHFR has been shown to exclude Cyclin B1 from the nucleus, resulting in the arrest of the cell cycle at around the G2 phase [7]. Other checkpoint regulators with an FHA domain, such as CHK2 and NBS1, have also shown similar features and arrest the cell cycle in response to DNA damage and replication blocks [8,9].

These checkpoint proteins containing FHA domain have been shown to function as tumor suppressors, although the detailed molecular mechanisms are not yet fully elucidated. For example, the inactivation of the CHK2 and NBS1 proteins increases the predisposition of cells to cancer development [8,10–14]. The functional inactivation of CHFR due to promoter methylation and the consequent loss of mRNA expression is frequently observed in human colon and gastric cancers [4,15–19], suggesting its possible role also as a tumor suppressor. The functional loss of these checkpoint proteins is likely to disrupt the cell cycle arrest response to cellular stress, thus leading to the accumulation of mutations and replication errors in the genome, a prerequisite for malignant transformation.

The RING-finger domain is a characteristic feature of the E3 ligase proteins [1] and is thought to determine the substrate specificity for ubiquitination reactions. As an example, the RING-finger protein cdc20 is known to serve as an E3 ligase for the anaphase promoting complex/cyclosome (APC/C) [20], and Cyclin B is also one of its substrates [20]. Cyclin B proteins that have been polyubiquitinated by cdc20 are rapidly transferred to the proteasome and degraded. CHFR was shown to play a role as E3 ligase for the polyubiquitination of Aurora A and Polo-like-kinase 1 [21,22], possibly resulting in the degradation of these proteins. In fact, mouse embryonic fibroblasts (MEF) derived from *Chfr* knockout mice show elevated protein levels of Aurora A and display chromosome abnormalities [21]. The inactivation of CHFR may thus cause the up-regulation of these proteins, which are known mitotic kinases and are frequently observed to be overexpressed in various types of human malignant tumors, such as bladder and colon cancers [23,24]. Elevated levels of Aurora A and Plk1 are known to induce abnormal mitotic cell division and

cause karyotype abnormalities or malignant transformation [25,26]. The functional loss of CHFR could therefore result in the accumulation of oncogenic proteins (Aurora A and Plk1) and induce genomic instability.

To date, two possible molecular pathways have been considered as the mechanisms underlying the tumor suppressor function of CHFR. These are the checkpoint regulation and E3 ligase functions of this protein. However, it is difficult to draw any conclusions from the findings of previous studies about which of these roles is the most critical for growth suppression, since functional analyses of the checkpoint and E3 ligase activity of CHFR have only been performed independently of each other thus far [1,22,27–29]. We initially focused on the E3 ligase activity as a possible pathway for the growth suppressive properties of CHFR as our previous data have shown that degradation by the proteasome is the major rate limiting step in the control of the Aurora A protein levels [30]. If the E3 ligase activity of CHFR is more important for growth suppression, as we initially expected, the core region of this tumor suppressor that is required for its anti-proliferative effects was anticipated to be the RF domain.

In our current study, we have investigated the molecular pathways underlying the growth suppressive functions of CHFR by utilizing genetic rescue experiments with colon cancer cell lines in which endogenous CHFR is epigenetically inactivated.

Materials and Methods

CHFR plasmids

A cDNA fragment of human CHFR (NIH Mammalian Gene Collection ID: 19963) was obtained by RT-PCR from a human pancreatic cancer cell line (Panc1) based on a method described previously [30]. A hemagglutinin (HA) protein tag sequence was then introduced at the amino terminus of this recombinant CHFR product and a Kozak sequence was inserted just upstream of the start codon of the HA protein tag. Mutant cDNA fragments were created using the quick change PCR kit (Stratagene) with slight modifications [31]. To generate a *Δ*FHA mutant, a CHFR cDNA fragment was generated that lacked the 110 amino acids between the original start methionine and the end of the FHA domain (MERPEEGKQS-EPEHNVAYLYESLS). An RF mutant (*Δ*RF) was similarly designed by generating a truncated CHFR cDNA lacking this 48 amino acid domain (CHCQDLLHD-TCRCPVERICK). A TGA stop codon was inserted into the CHFR cDNA to construct the cysteine rich domain mutant (*Δ*Cys) by producing a protein product lacking the 190 amino acids of this region (VCPLQGSHAL-HICEQTRFKN).

Each cDNA was subcloned into the EcoRV site of pBluescript SKII+ (Stratagene) by blunt end ligation, and the resulting constructs were validated in a cycle sequencing reaction with an ABI 310 genetic analyzer (Applied Biosystems). Both the wild-type and mutant CHFR cDNA fragments were also subcloned into an LXIN retrovirus vector (Clontech), the pcDNA 3.1+ plasmid (Invitrogen), and an IRES2-EGFP bicistronic expression vector (Clontech). The retrovirus vectors were used in colony formation assays, whereas the pcDNA 3.1+ vectors were used in an *in vivo* ubiquitination assay and also in the cellular localization experiments. The bicistronic vectors (IRES2-EGFP) were employed in the checkpoint analyses.

Stable and transient expression of wild-type and mutant CHFR proteins in cultured cells

HCT116, RKO and HeLa cells were cultured in Dulbecco's Modified Eagle's Medium (DMEM; Sigma) supplemented with 10% fetal bovine serum (FBS), penicillin (100U/ml), and streptomycin (50U/ml), at 37°C and 5% CO_2. A PT67 retrovirus packaging cell line was obtained from Clontech, and maintained in DMEM with 10% FBS. Cells were maintained in an exponential growth phase prior to use.

Retroviral constructs harboring wild-type or mutant human *CHFR* cDNAs, were introduced into PT67 cells (Clontech) for packaging using the lipofection method (Fugene 6, Roche). The LXIN retroviral vector contains a neomycin cassette, and cells that stably produced recombinant retroviruses were selected after two weeks of culture in the presence of 1 mg/ml G418. The retroviral supernatants were diluted 1:2 with normal DMEM containing 10% FBS and exposed to HCT116 or RKO cells with 400 μg/ml of polybrane infection enhancer. Infected cells were further selected with 1 mg/ml G418 for two weeks. To avoid cloning bias, the whole cell population that showed resistance to G418 was used in each experiment. For transient expression experiments, cells at 70% confluency were transfected with 2.5 μg of the indicated plasmids using the lipofection method (Lipofectamine 2000, Invitrogen), according to the manufacturer's protocol.

Colony formation assay

1×10^6 HCT116, RKO or HeLa cells were infected with aliquots of LXIN retroviral supernatants from the PT67 packaging cells for 48 h. When the infected cells reached confluence, they were trypsinized and resuspended in 10 ml of DMEM supplemented with 10% FBS. 10 μl (HCT116) or 100 μl (RKO or HeLa) aliquots of these cell suspensions were then seeded into 100 mm culture dishes (Nunc, 150350), and grown in G418 selection for two weeks as described above. G418-resistant colonies were subsequently fixed in 4% paraformaldehyde in phosphate buffered saline (PBS), and stained with hematoxilin. Images of the stained dishes were captured using a high-resolution digital camera with a macro lens (Fuji Film), and the numbers of colonies were determined in each image using NIH image software. The average colony numbers were then calculated from five dishes in three independent experiments. Statistical significance was evaluated with the Wilcoxon-Mann-Whitney *U*-test.

Measurement of the retrovirus titers of the producer cells

The conditioned medium of the producer cells was diluted 1:50 with distilled water and subjected to reverse transcription. The copy number of the resulting retroviral cDNA was measured by real-time PCR with a Retrovirus titer set (Takara Bio, Kyoto, Japan). The average retrovirus copy number of per ml was determined from five independent reactions. The reverse transcriptase and real-time PCR reactions were performed according to the manufacturer's instructions.

Western blot analysis

Cells were lysed in ice-cold HIPS buffer (50 mM Tris-HCl, pH 7.5, 150 mM NaCl, 1% Triton X-100) [30] and the resulting whole cell lysates were subjected to 10% SDS-PAGE. The separated proteins were then transferred to polyvinylidene difluoride (PVDF) membranes (Immobilon P, Millipore). After blocking with 7% non-fat dry milk-Tris buffered saline and 0.1% Tween 20 (TBST), the membranes were probed with anti-HA (High affinity HA 3F10, 1/5,000 dilution, Roche), and anti-α-tubulin (DM-1A, 1/5,000 dilution, ICN Biomedicals) antibodies. Blots were then incubated with horseradish peroxidase (HRP)-conjugated rabbit anti-rat IgG (A5795, 1/5,000 dilution, Roche) or donkey anti-mouse IgG (NA1093V, 1/5,000 dilution, GE Healthcare Bioscience) secondary antibodies respectively, and immunoreactive proteins were detected by enhanced chemiluminescence (P90720, Millipore).

In vivo ubiquitination assay

2.5 μg of wild-type and mutant CHFR pcDNA 3.1+ expression plasmids, and an empty vector control, were introduced into HCT116 cells at 70% confluency using the lipofection method (Lipofectamine 2000, Invitrogen). 2.5 μg of pcDNA 3.1+ vector harboring FLAG tagged ubiquitin (kindly provided by Dr. K. Miyazono, Tokyo University) was co-transfected with these constructs. After 20 h, the cells were treated with 25 μM of MG132 (C2211, SIGMA) for 5 h, lysed in HIPS buffer, and subjected to immunoprecipitation. A 500 μg aliquot of total protein from the transfected HCT116 cells in 250 μl lysis solution was mixed with 10 μl of the anti-HA affinity matrix (Roche) pre-blocked with 2% bovine serum albumin (BSA), and incubated for 4 h with gentle rotation at 4°C. The affinity matrix was washed with HIPS buffer three times, collected by centrifugation, and the precipitated proteins were denatured in sample buffer containing 0.1M dithiothreitol (DTT), subjected to 7% SDS-PAGE and transferred to a PVDF membrane. The transferred proteins were then incubated with anti-HA (high affinity HA 3F10, 1/5,000 dilution, Roche), or anti-FLAG (monoclonal anti-FLAG M2, 1/5,000 dilution, Sigma) antibodies. The secondary antibodies used were as described above for the western blotting procedure.

Intracellular localization of CHFR protein

pcDNA3.1+ expression vectors were introduced into HCT116 cells using the lipofection method, as described earlier. Twenty-four hours after transfection, the cells were fixed with 4% paraformaldehyde and then treated with 0.5% Triton X-100 (both in PBS) for 5 min. The cells were preblocked with 1% normal goat serum (NGS) in PBS for 30 min and incubated with an anti-HA antibody (high affinity HA 3F10, 1:500 dilution, Roche) for 1 h at room temperature. An alexa 488-conjugated goat anti-rat IgG (Invitrogen) was used as the secondary antibody. A rabbit PML antibody (PM001, 1/300 dilution, MBL) and alexa 594-conjugated goat anti-rabbit IgG (Invitrogen) were used to detect PML nuclear foci. The cells were counter-stained in each case with 1μM of Hoechst 33258 (B1155, Sigma) and staining images were captured using an Axiovart (Zeiss) fluorescence microscope.

Cell cycle checkpoint analysis

For checkpoint analysis, HCT116 cells were transfected with IRES2-EGFP expression plasmids harboring wild-type or mutant CHFR inserts for 5 h and then treated with nocodazole at a concentration of 200 ng/ml (from a 100 mg/ml stock solution in dimethyl sulfoxide, Sigma) for 16 h. After the nocodazole treatment, the cells were fixed in 4% paraformaldehyde/PBS and the numbers of mitotic cells, which show EGFP fluorescence, were determined by microscopic examination. The average percentage of the total EGFP-positive cells that were deemed to be mitotic was calculated by counting approximately 100 cells expressing either wild-type or mutant CHFR proteins.

Results

The expression of wild-type and mutant CHFR proteins in colon cancer cells which lack the endogenous species

Colon cancer cells have lost the endogenous expression of CHFR, and we thus anticipated that this would be an appropriate cell system to elucidate the functional domain responsible for the anti-proliferative effects of CHFR protein by genetic rescue. The endogenous levels of *CHFR* mRNA were measured by real-time RT-PCR in five pancreatic cancer cell lines and six colon cancer cell lines (Fig. 1C). *CHFR* transcripts were detectable in each of the pancreas cell lines tested but three colon cancer derived cell lines, HCT116, RKO and DLD1, showed no expression of *CHFR* mRNA.

The structures of the wild-type and mutant CHFR proteins are shown in Figure 1A. Expression vectors for these proteins were introduced transiently into HCT116 cells and subjected to western blotting with anti-HA antibodies to determine whether the predicted recombinant CHFR proteins were produced (Fig. 1B). Positive bands were indeed detected at the expected molecular weights (wild-type; 72 kDa, ΔFHA; 57 kDa, ΔRF; 66 kDa, ΔCys; 50 kDa), indicating that each CHFR protein product was efficiently expressed.

The anti-proliferative effects of CHFR are dependent upon the FHA domain and not the RF or Cys domains

To evaluate the effects of wild-type and mutant CHFR proteins (ΔFHA, ΔRF and ΔCys) on cell proliferation, recombinant retroviruses harboring the corresponding cDNAs were introduced into HCT116 cells. There were no major differences found in the resulting cell morphologies in each case, as shown in Figure 2A. Substantial growth suppression was observed following the introduction of the wild-type CHFR during G418 selection (Fig. 2A). In addition, whereas the ΔRF and ΔCys mutants showed growth suppressive effects that were almost identical to the wild-type CHFR, the ΔFHA protein had minimal inhibitory effects upon cell proliferation (Fig. 2A).

To more quantitatively evaluate the growth inhibitory effects of the wild-type and mutant CHFR proteins, a colony formation assay was carried out using the corresponding retrovirally infected HCT116 cells under G418 selection (Fig. 2B and C). The expression of wild-type, ΔRF and ΔCys proteins resulted in a significant decrease in the number of G418-resistant colonies in this experiment compared with the vector control ($p<0.01$), whereas ΔFHA expressing cells did not show any reduction in colony number. The same recombinant *CHFR* retroviruses were also introduced into RKO cells and similar results were observed (Fig. 2C).

To verify the titer of our recombinant CHFR retroviruses, the virus copy numbers in the conditioned supernatant of the PT67 producer cells were measured by real-time PCR. As shown in Figure 2D, no major differences could be observed in the retrovirus copy number between the wild-type and mutant CHFR retrovirus producer cells. We therefore concluded that the growth suppressive effects of CHFR that we observed in these analyses are not due to any differences in the titers of the producer cells.

Detection of wild-type and mutant CHFR proteins under stable expression conditions

During their initial passages, significant growth suppression was observed in HCT116 cells expressing exogenous wild-type, ΔRF and ΔCys CHFR, as shown in Figures 2A–C. However, this growth suppression becomes almost undetectable by passage 3. The protein levels of each of these introduced CHFR products were thus analyzed in these cells at passage 4 by western blotting. As shown in Figure 2E, the levels of the wild-type, ΔRF and ΔCys products were remarkably low when compared with ΔFHA (Fig. 2E, left panel). The same analysis was undertaken in RKO cells and produced essentially identical results (Fig. 2E, right panel). A possible explanation for this phenomenon is that elevated levels of wild-type, ΔRF and ΔCys proteins may cause a substantial growth disadvantage, and thus cell populations which express these introduced proteins at low levels undergo positive selection with passage in culture.

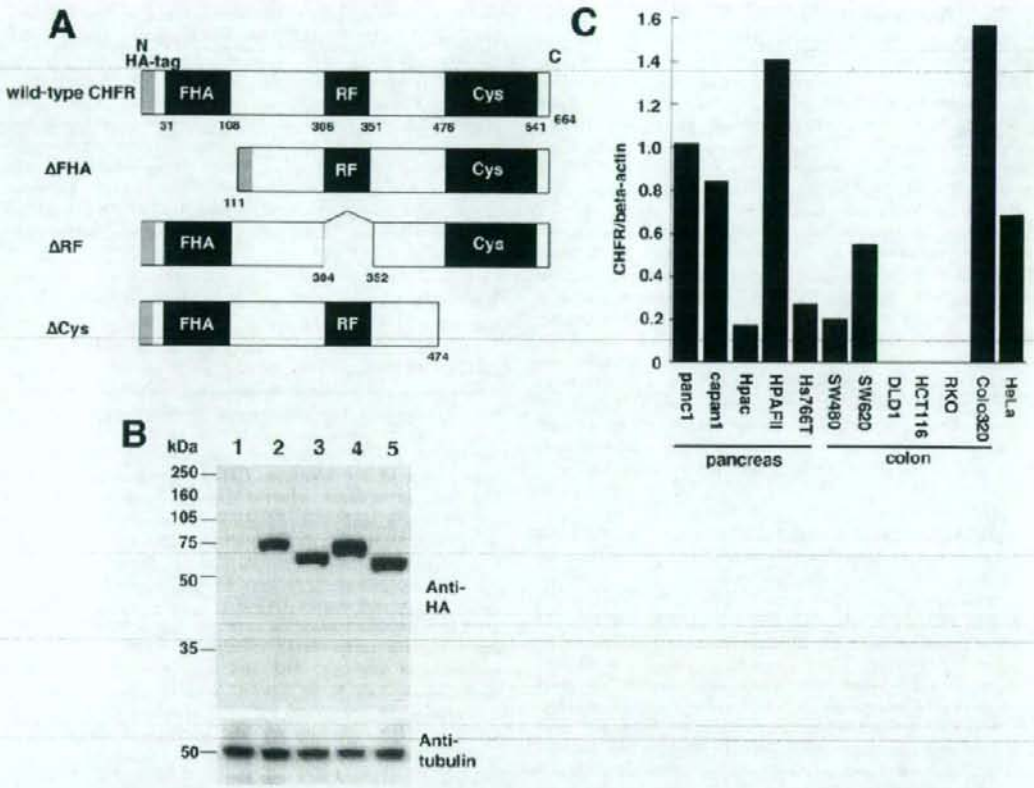

Figure 1. Schematic representation of the wild-type, ΔFHA, ΔRF and ΔCys forms of the CHFR protein tagged with HA, and expression analysis of these proteins in a colon cancer-derived cell line that lacks endogenous CHFR mRNA. (A) The predicted protein structures of the wild-type, ΔFHA, ΔRF and ΔCys CHFR proteins. N and C indicate the amino and carboxyl terminus, respectively. FHA, forkhead associated domain; RF, ring finger domain; Cys, cysteine rich domain; HA-tag, hemagglutinin protein tag. (B) The detection of the wild-type, ΔFHA, ΔRF and ΔCys forms of CHFR proteins transiently expressed in HCT116 cells by western blotting with anti-HA antibodies (upper panel). Cells were transfected with HA-tagged empty vector (lane 1); wild-type CHFR (lane 2); ΔFHA (lane 3); ΔRF (lane 4); or ΔCys (lane 5). Tubulin was also detected as a loading control (lower panel). (C) Endogenous CHFR mRNA expression levels detected by real-time PCR in the indicated pancreatic- and colon cancer-derived cell lines. The relative levels of CHFR mRNA shown are normalized to beta-actin mRNA, the expression level of panc1 was set as 1.0, and the average values of duplicate experiments were calculated.
doi:10.1371/journal.pone.0001776.g001

The E3 ligase activity of CHFR requires the RF and Cys domains, but not the FHA domain

A series of *in vivo* ubiquitination assays were conducted using HCT116 cell populations that transiently expressed the wild-type and mutant CHFR proteins at similar levels (Fig 3, left panel). The recombinant CHFR and its substrate proteins were immunoprecipitated from the corresponding cellular extracts with an anti-HA antibody and the ubiquitination activity levels were then monitored by western analysis with anti-FLAG antibodies to detect high molecular weight bands as described in a previous study [32]. As shown in the right panel of Figure 3, polyubiquitinated proteins were detectable in cells expressing wild-type and ΔFHA proteins but not the ΔRF and ΔCys mutants, which is deemed to be substrates of CHFR. The mobilities of these immunoprecipitated CHFR proteins were also not altered as a result of polyubiquitination (Fig. 3, middle panel), indicating that no self-ubiquitination had occurred in each case. From these results, we concluded that E3 ligase activity of CHFR requires the RF and Cys domains, but is unaffected by the deletion of the FHA domain.

Analysis of the intracellular localization of wild type, ΔFHA, ΔRF and ΔCys CHFR proteins by immunofluorescence staining

A previous study has indicated that the FHA domain of the CHFR protein is essential for its localization in promyelocytic leukemia (PML) foci within the nucleus [33]. The intracellular localization of the wild type and mutant CHFR proteins was detected by immunostaining of HCT116 cells that exogenously expressed these products. As shown in Figure 4, each of these

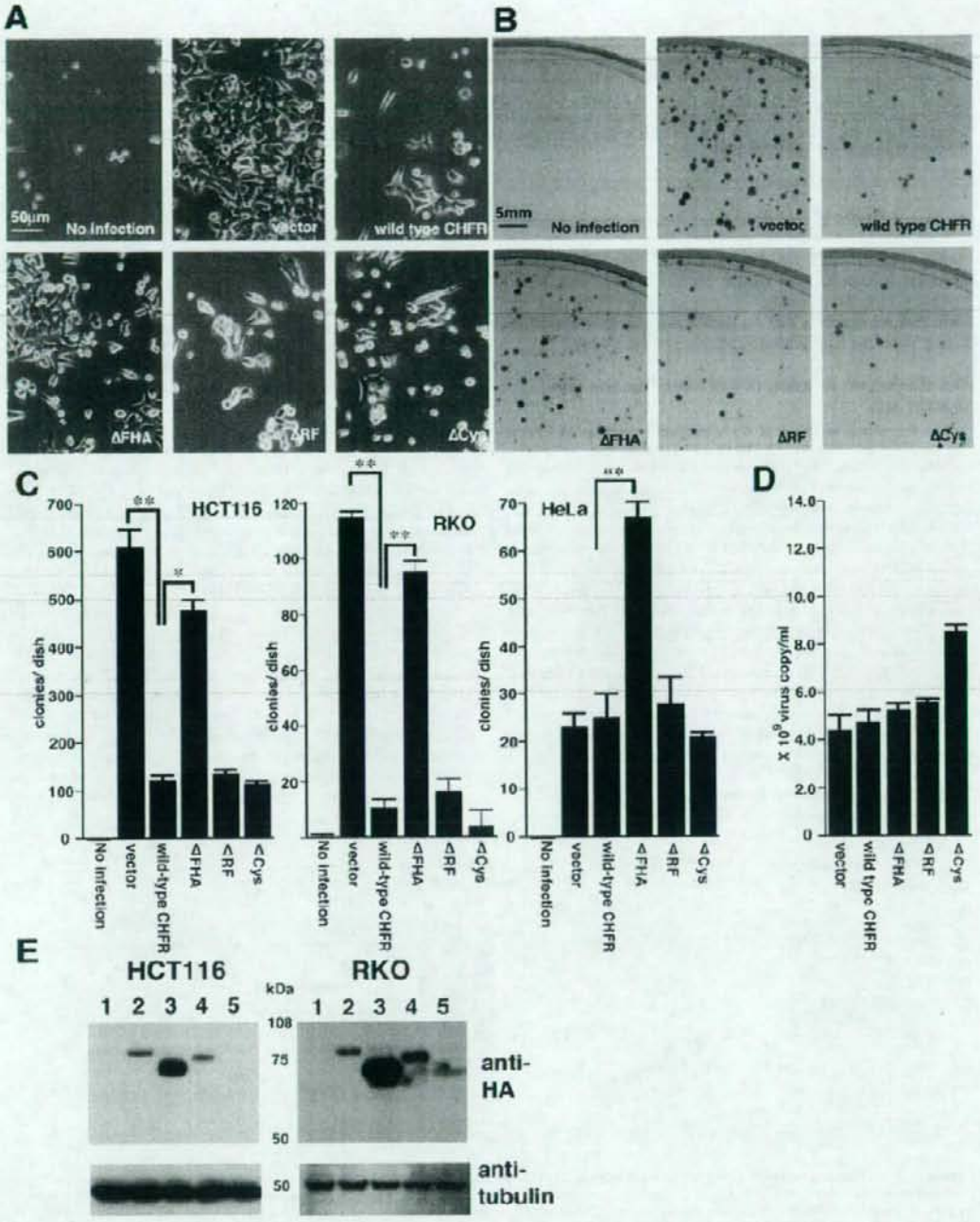

Figure 2. Identification of the functional domain of the CHFR protein that confers its anti-proliferative effects. (A) The growth appearance of HCT116 cells infected with retroviral vectors expressing the indicated CHFR products. Note that the wild-type CHFR, ΔRF and ΔCys retroviruses suppressed the cell growth of the host cells and this was partially restored in the ΔFHA expressing cells. There were no differences,

←

however, between any of these transfected cells in terms of their morphology. (B) Colony formation assay of HCT116 cells after retroviral infection with the same CHFR constructs as in (A). (C) Statistical evaluation of the colony formation assay results for HCT116, RKO and HeLa cells expressing the indicated exogenous proteins. *p<0.01, **p<0.05. (D) Measurements of the recombinant retrovirus copy number in the supernatants of PT67 producer cells by real time PCR. (E) The detection of stably expressed wild-type, ΔFHA, a ΔRF and ΔCys CHFR protein in HCT116 and RKO cells following infection with the corresponding recombinant retroviruses. Total cellular protein extracts were obtained at the fourth passage. The level of introduced proteins in the cells that infected with empty vector (lane 1); wild-type CHFR (lane 2); ΔFHA (lane 3); ΔRF (lane 4); or ΔCys (lane 5).
doi:10.1371/journal.pone.0001776.g002

introduced CHFR species showed a diffuse nuclear localization and no differences could be observed. Although the cells were doubly stained with anti-HA and anti-PML antibodies, a dominant accumulation of CHFR within the PML nuclear foci was not evident for either the wild type or mutant proteins. From these data, we conclude that the CHFR domains analyzed do not impact upon the intracellular localization of this protein.

The checkpoint function of CHFR requires the FHA domain only

The functional recovery of the checkpoint function of CHFR was evaluated also in HCT116 cells after the exogenous introduction of wild type and mutant CHFR proteins. Since the transfection efficiency was limited to around 5% for the transient expression vector, a bicistronic expression vector harboring the CHFR wild type and mutant inserts was used in these experiments (Fig. 5A). Since in this case the CHFR and EGFP protein products are translated from the same mRNA, EGFP fluorescence can be used as a marker of recombinant CHFR protein expression. To validate the positive correlation between EGFP expression and CHFR expression, the percentage of EGFP positive cells that were immunoreactive also for the anti-HA antibody was determined microscopically (Fig 5B). Among the 200 EGFP-positive cells that were counted, 182 (91%) showed positive staining for anti-HA antibody (Fig. 5B), confirming the usefulness of EGFP as a marker. As shown in Figure 5C, following nocodazole treatment, the percentage of EGFP-positive mitotic cells was found to decrease in conjunction with the expression of the wild type, ΔRF and ΔCys CHFR proteins, compared with the vector control. In contrast, the expression of the ΔFHA mutant did not affect the percentage of mitotic cells. From these data, we conclude that the FHA domain is essential for the mitotic checkpoint function of CHFR.

Discussion

Our current study has identified the CHFR domains that are responsible for the anti-proliferative effects of this protein and the results are summarized in Table 1. We find that both the anti-proliferative effects and checkpoint function of CHFR require the FHA domain, whereas the E3 ligase activity of this tumor suppressor relies on the RF and Cys domains. This suggests that there is a functional link between the anti-proliferative effects and checkpoint function of CHFR. Our present analyses also reveal that the FHA domain is the most important region of CHFR for its anti-proliferative role, which is in good agreement with several previous studies. Toyota *et al* have also reported that the introduction of a wild-type CHFR expression vector causes the growth suppression of the host cells, whereas a FHA deletion mutant did not affect cell growth [19].

Although the data presented by Toyota *et al* was quite suggestive of the essential role of FHA in cell growth control, it should be noted that the cell lines they analyzed (SW480 and T98G) endogenously express CHFR transcripts (see Fig. 1C for SW480) [34]. The accurate and quantitative evaluation of the impact of the ΔFHA mutant on cell growth is difficult to undertake in the presence of endogenous protein because of the dominant-negative properties of this mutant [1]. Interestingly, we detected that the expression of these mutant CHFR proteins had a completely different result upon the growth of HeLa cells, which express

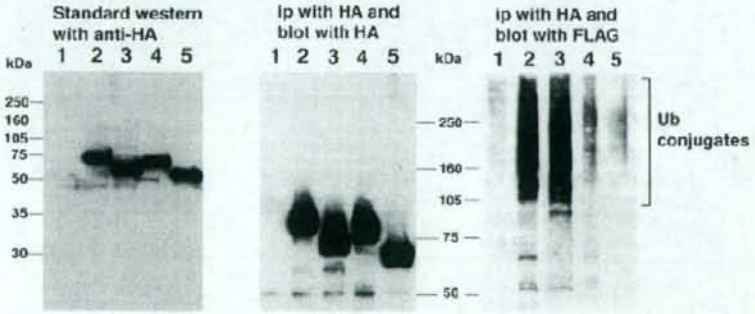

Figure 3. *In vivo* ubiquitination assay for the wild-type, ΔFHA, ΔRF and ΔCys forms of the CHFR protein. (Left panel) Measurement of the transient expression levels of both the wild-type and mutant form of CHFR proteins in HCT116 cells by western blotting. The proteins were separated by 10% SDS-PAGE. (Middle panel) Immunoprecipitation and immunoblotting of proteins with anti-HA antibodies. The proteins were resolved by 7.5% SDS-PAGE. (Right panel) The detection of FLAG-reactive proteins following immunoprecipitation by HA antibodies. Ubiquitinated proteins are evident by the presence of high molecular weight bands in lanes 2 and 3, but not in lanes 1, 4 and 5. Cells were cotransfected with FLAG tagged ubiquitin expression (FLAG-Ubi) vector and either empty vector (lane 1); wild-type CHFR (lane 2); ΔFHA (lane 3); ΔRF (lane 4); or ΔCys (lane 5).
doi:10.1371/journal.pone.0001776.g003

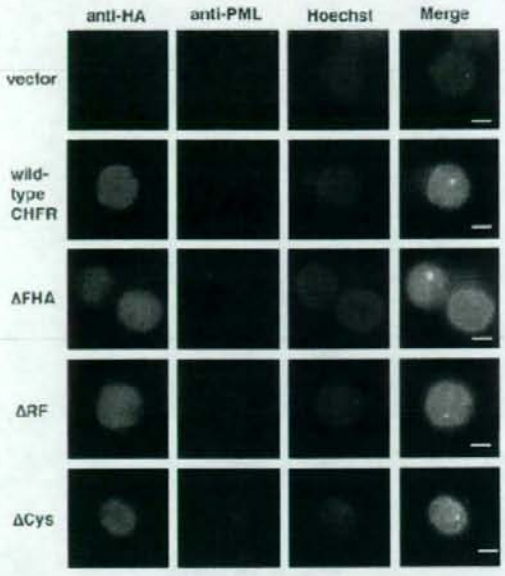

Figure 4. Intracellular localization of wild-type and mutant forms of CHFR proteins detected by fluorescence immunostaining. The localization of the wild-type or mutant forms of the CHFR protein was assessed by the immunoreactivity of an anti-HA antibody (green signal). PML nuclear foci were detected with an anti-PML antibody (red signal). The nuclei of HCT116 cells were counterstained with Hoechst (blue). Merged pictures are shown to highlight the signal overlap between the Hoechst and anti-HA staining.
doi:10.1371/journal.pone.0001776.g004

endogenous CHFR, compared with HCT116 and RKO cells (Fig. 2C). In these experiments, the expression of ΔFHA induced a significant increase in colony number whereas the wild-type, ΔRF and ΔCys CHFR species did not show any effects (Fig. 2C, Right panel). A previous study has indicated that the ΔFHA mutant of CHFR acts as a dominant-negative and can disrupt the checkpoint function of the wild type protein [1]. Hence, we speculated that the increase in the colony number in HeLa cells by ΔFHA was caused by the dominant-negative effects of this mutant upon the endogenous wild type CHFR protein [1]. The reported existence of a splicing variant form of CHFR that lacks the FHA domain and acts in a dominant-negative manner further supports our contention [19]. It has not yet been reported until this manuscript to evaluate the effect of FHA domain against cell proliferation under the two conditions, the existence and non-existence of endogenous CHFR. We therefore conclude that our current study is the first report that precisely identifies the functional domain responsible for the anti-proliferative function of CHFR.

We show from our analysis that the loss of the RF domain and its associated E3 ligase activity did not disrupt the anti-proliferative effects of CHFR, suggesting that the E3 ligase activity of this protein is not essential for its tumor suppressor function. From previous functional analysis of CHFR knockout mice, however, Yu *et al* concluded that the tumor suppressor function of CHFR is conferred by its E3 ligase activity toward the Aurora A protein, a predicted oncogenic kinase [21]. There is therefore some disagreement regarding the precise role of the E3 ligase activity of CHFR, but possible explanation can be considered. We need to pay attention to the tissue specificity of CHFR to induce the degradation of Aurora A. Elevated protein levels of Aurora A are frequently observed in both human colon and mammary cancers [25,26], but the inactivation of CHFR is limited to cases of colon cancer [17,35]. High levels of Aurora A in mammary cancers cannot therefore be explained by a loss of function of CHFR. These findings indicate the existence of degradation pathways for Aurora A that are independent of CHFR [17]. In this regard, Cdh1 is a strong candidate as an alternative E3 ligase for Aurora A [36,37]. The exogenous introduction of a dominant-negative form of Cdh1 was reported to induce elevated levels of Aurora A protein in HeLa cells [37]. Hence, there may be several molecular pathways that promote the degradation of Aurora A but that are tissue- or organ-specific. The protein levels of Aurora A did not change after the expression of any form of CHFR in HCT116 colon cancer cells in our current experiments (data not shown). The differences between the findings of this and other studies might thus be due to the cell-type specificity of the degradation pathways for Aurora A.

With regards to the E3 ligase activity of CHFR, we found that the RF and Cys domains are essential. These results are consistent with previously reported findings, which show that CHFR binds to its substrates through its Cys domain, and forms a protein complex with APC/C through its RF domain [21]. Some E3 ligases have also been reported to have self-ubiquitination activity [38,39], but we did not detect this in the case of CHFR. In contrast, Kang *et al* have reported strong self-ubiquitination activity for CHFR [22]. One possibility to be taken into consideration when evaluating these discrepancies is the difference of their GST protein tag and our HA tag. The self ubiquitination activity affected by the protein tag has reported with MBP protein tag in case of Rma1, E1.5 and Perkin [40–42]. Therefore, further experiments with other protein tags would be needed to get the conclusion about the self ubiquitination activity of CHFR protein.

The results of our current study also show that the expression of CHFR arrests the cell cycle prior to entry into mitosis in the presence of microtubule depolymerizing reagents, which is consistent with previous reports [1,19,22,27,28]. A growth advantage will be conferred upon cells which have lost the checkpoint machinery that functions under mitotic stress conditions. In agreement with this idea, shRNA knock down of CHFR recently reported to induce the increased cell proliferation during the preparation of this manuscript [43]. Since the promoter methylation of the *CHFR* gene was detected in non-invasive adenoma lesions of colon epithelia [44], the associated loss of the checkpoint function of CHFR in these cells may have a significant impact upon the early stages of colon carcinogenesis. To gain further supportive evidence that the FHA domain of CHFR is important for its growth inhibition properties, we have recently put a considerable amount of effort into establishing a conditional expression system for this protein using the Cre-loxP recombination system [30] to evaluate tumor formation activity *in vivo* (e.g. nude mice). Unfortunately, we have yet to establish an efficient conditional system due to the toxicity of Cre-expressing adenovirus in HCT116 colon cancer cells. Although it is not direct evidence, a remarkably high protein level of the ΔFHA mutant, compared with that of the wild-type and other mutant forms of CHFR, suggests that the FHA domain has an important role in suppressing tumor formation (Fig. 2E). The FHA domain is expected to work as the binding motif for phosphorylated proteins. We are currently working on the experiments to isolate the binding partner of FHA domain of CHFR protein. There is a possibility that the detail of anti-